OK

NBS

Technical Note 165

FADING CORRELATION BANDWIDTH AND SHORT-TERM FREQUENCY STABILITY MEASUREMENTS ON A HIGH-FREQUENCY TRANSAURORAL PATH

J. L. AUTERMAN

U. S. DEPARTMENT OF COMMERCE
NATIONAL BUREAU OF STANDARDS

THE NATIONAL BUREAU OF STANDARDS

Functions and Activities

The functions of the National Bureau of Standards are set forth in the Act of Congress, March 3, 1901, as amended by Congress in Public Law 619, 1950. These include the development and maintenance of the national standards of measurement and the provision of means and methods for making measurements consistent with these standards; the determination of physical constants and properties of materials; the development of methods and instruments for testing materials, devices, and structures; advisory services to government agencies on scientific and technical problems; invention and development of devices to serve special needs of the Government; and the development of standard practices, codes, and specifications. The work includes basic and applied research, development, engineering, instrumentation, testing, evaluation, calibration services, and various consultation and information services. Research projects are also performed for other government agencies when the work relates to and supplements the basic program of the Bureau or when the Bureau's unique competence is required. The scope of activities is suggested by the listing of divisions and sections on the inside of the back cover.

Publications

The results of the Bureau's research are published either in the Bureau's own series of publications or in the journals of professional and scientific societies. The Bureau itself publishes three periodicals available from the Government Printing Office: The Journal of Research, published in four separate sections, presents complete scientific and technical papers; the Technical News Bulletin presents summary and preliminary reports on work in progress; and Basic Radio Propagation Predictions provides data for determining the best frequencies to use for radio communications throughout the world. There are also five series of nonperiodical publications: Monographs, Applied Mathematics Series, Handbooks, Miscellaneous Publications, and Technical Notes.

A complete listing of the Bureau's publications can be found in National Bureau of Standards Circular 460, Publications of the National Bureau of Standards, 1901 to June 1947 ($1.25), and the Supplement to National Bureau of Standards Circular 460, July 1947 to June 1957 ($1.50), and Miscellaneous Publication 240, July 1957 to June 1960 (Includes Titles of Papers Published in Outside Journals 1950 to 1959) ($2.25); available from the Superintendent of Documents, Government Printing Office, Washington 25, D. C.

(5)-603 300

NATIONAL BUREAU OF STANDARDS

(11)- **Technical Note**
165

(9)-OCT[redacted]962

(7) N.A.
(10) 53p incl. illus. table, 15 refs.
(12) N.A.
(13) N.A.

(6)-FADING CORRELATION BANDWIDTH AND SHORT-TERM FREQUENCY STABILITY MEASUREMENTS ON A HIGH-FREQUENCY TRANSAURORAL PATH

(8)-James L. Auterman
Boulder Laboratories
Boulder, Colorado

NBS Technical Notes are designed to supplement the Bureau's regular publications program. They provide a means for making available scientific data that are of transient or limited interest. Technical Notes may be listed or referred to in the open literature.

For sale by the Superintendent of Documents, U.S. Government Printing Office
Washington 25, D.C. - Price 40 cents

FOREWORD

The studies reported herein were carried out on behalf of the U. S. Air Force under support of the Electronic Systems Division, Air Force Systems Command, L. G. Hanscom Field (PRO 61-545). Part of the analysis and the publication of this report was supported by NBS Research and Technical Service program, Project 85141.

CONTENTS

Fading Correlation Bandwidth and Short-Term Frequency Stability Measurements on a High-Frequency Transauroral Path

James L. Auterman

ABSTRACT

Measurements of fading correlation bandwidth and of deviations of the instantaneous frequency from the average carrier frequency were made on the 4500-km auroral path from Barrow, Alaska, to Boulder, Colorado, at frequencies near 15 and 20 Mc/s.

The mean fading correlation bandwidth was found to be 4.3 kc/s. The value exceeded 90% of the time was 1.0 kc/s; the value exceeded 10% of the time was not obtainable. Generally, the bandwidth was smaller during periods of high magnetic activity or high fade rate. It also exhibited a minimum near midday.

Cumulative distributions of instantaneous frequency deviations were obtained for a variety of conditions. The distributions generally agreed with a theoretical distribution based on a narrow-band Gaussian noise model if the proper normalizing factor was used. The factor was 1.4 times the measured fade rate. Distributions were also obtained of the percent of time the frequency deviations exceeded certain values for various time durations. Several examples of each type of distribution are presented.

1. INTRODUCTION

In recent years rapid advances have been made in the field of communication theory. Many hypothetical and a few practical communication systems have been analyzed. Generally, it has been assumed that amplitude fading of the signal was Rayleigh distributed, the additive noise was Gaussian, and the channel was phase coherent. Occasionally other statistical forms have been used,but the above assumptions usually were made because they were well-known, were similar to the characteristics of some real channel, and were mathematically tractable.

In order to apply communication theory to a practical channel, one must have a knowledge of the short-term statistics of the channel. Statistical knowledge of HF radio propagation is very limited. This report describes measurements of the correlation between the fading envelopes of two carriers closely spaced in frequency (from which information on the fading correlation bandwidth can be obtained), and discusses the short-term fluctuations in the instantaneous frequency of the received carrier signal. These short-term fluctuations are due to Doppler shifts produced by ionospheric changes and the result of beating together of multipath components.

All of the measurements were made on the 4470-km transauroral path from Barrow, Alaska,to Boulder, Colorado,at carrier frequencies of 14.688 Mc/s and 19.247 Mc/s. Figure 1 shows the location of the path relative to the auroral zone. This is typically a two-hop path for the frequencies used, although on occasion electron densities may be high enough to support three-hop propagation. One-hop propagation of the Pederson ray is also possible, but it is usually much lower in amplitude than the dominant two-hop mode, so its effect on the measurements is probably insignificant.

2. EXPERIMENTAL FACILITIES COMMON TO BOTH EXPERIMENTS

The transmitters were located at the Arctic Research Laboratories Camp at Barrow, Alaska, and were operated at a nominal 2-kw output.

Carrier frequency stability was maintained at about one part in 10^8 by high-quality crystal oscillators. The transmitting antennas were quarter-wave monopoles.

The receiving facilities were located at the National Bureau of Standards Table Mesa Field Site, approximately ten miles north of Boulder, Colorado. The receiving antenna was either a half-wave dipole, one wavelength above ground, or a Signal Corps Type A rhombic antenna. All antennas were oriented on the great-circle path to Barrow.

High-quality communication receivers were used with all receiver oscillators crystal-controlled and having stabilities comparable to those of the transmitted frequency. Triple conversion was used to obtain a 10-kc/s IF which was available for recording on magnetic tape or other processing (see figure 2).

Continuous strip chart records of field strength and fading rate were also made in order to facilitate later data analysis. The receiving and recording equipment was essentially the same as that used previously by others at NBS [Koch and Petrie, 1962; Koch and Beery, 1962].

3. FADING CORRELATION BANDWIDTH

Fading correlation bandwidth is defined as the frequency spacing at which the normalized correlation coefficient of the envelopes of two cw carriers falls to 0.5. In this experiment correlation bandwidth was measured by plotting a curve of envelope correlation versus frequency spacing.

In the transmission of analog information it is usually desired to have a flat frequency response over the band occupied by the signal. The fading correlation bandwidth is a measure of how well this is achieved. In some systems diversity reception is used to obtain improved performance. The improvement is not significant unless the correlation between channels is on the order of 0.6 or less [Staras, 1956]. The fading correlation bandwidth would be indicative of the frequency spacing needed in a frequency diversity scheme.

Fading of an HF carrier is due to two principal causes, slow fading due to changes in absorption and faster fading due to interference among the multipath components. The absorption will affect all frequencies within normal HF communication bandwidths in a similar manner, whereas the multipath interference will result in fading which, in general, will not occur simultaneously over the frequency band of interest. This effect is called selective fading and is the heart of the fading correlation bandwidth problem.

3.1. A Theoretical Model

No complete theoretical analysis of the fading correlation problem has come to the author's attention although estimates have been made based on a simplified model [Staras, 1958]. If one assumes that the received signal contains two phase-coherent multipath components with a path-length difference corresponding to D seconds and a frequency such that the difference corresponds to a multiple wavelength, the two components will add in phase. At other frequencies, such that D corresponds to an odd multiple of a half-wavelength, the two signals will arrive out of phase and cancel. Thus minima and maxima occur alternately as the frequency is varied, the spacing between adjacent minima and maxima being $\frac{1}{2D}$ and from maxima to maxima or minima to minima being $\frac{1}{D}$. The frequencies at which maxima and minima occur are assumed to vary due to slight changes in the differential time delay, resulting in fading at any particular frequency as the maxima and minima move past. In the case of HF propagation, this is assumed to be caused by changes in the ionosphere.

Over bandwidths that are small compared to the reciprocal of the delay difference, fading will be well correlated. At frequency spacings on the order of $\frac{1}{2D}$, i.e., the maxima to minima spacing, one would expect negative correlation. The correlated bandwidth would then be somewhat less than $\frac{1}{2D}$. Using this simplified model, one would also expect good correlation at frequency spacings of multiples of $\frac{1}{D}$ and poor correlation at odd multiples of $\frac{1}{2D}$. Then the correlation as a function of frequency spacing would have an oscillatory component of period $\frac{1}{D}$.

An HF communication channel is frequently more complicated than the model just described. The multipath components do not, in general, traverse exactly the same portions of the ionosphere and, therefore, are affected independently by the smaller ionospheric perturbations. This introduces a randomness which obscures the well-defined multipath components of the model. Scatter propagation would be an extreme example of this, since in the scatter mode there are many multipath components and a continuum of multipath delays. This would destroy any periodicity in the correlation function, and one would expect the correlation to be a monotonically decreasing function of frequency spacing, eventually vanishing for sufficiently wide spacings. This is indicated in the brief measurements made by Koch [1958] on ionospheric scatter propagation. Then, for HF propagation, one would expect the fading correlation coefficient to decrease with increasing frequency spacing with, perhaps, a periodic component, depending upon the number and coherence of the multipath components. The periodic portion of the correlation would be expected to decay at increased spacings. The fading correlation bandwidth would be inversely proportional to the multipath delay.

3.2. Experimental Results

The CW carriers at appropriate frequency spacings were obtained by modulating the AM transmitters at Barrow, Alaska with an audio tone. This yielded an output consisting of a 2-kw carrier and 360-watt sidebands displaced above and below the carrier by the audio tone. The modulation level was maintained at 85%. By using the carrier and a sideband or the two sidebands one could determine correlations for two frequency spacings simultaneously, i.e., spacings equal to the audio tone and twice the audio tone. Although it would have been desirable to have several frequency spacings available simultaneously, logistics and signal-to-noise ratio considerations prevented it.

The received signal was translated to a 10-kc/s IF and recorded on magnetic tape for later analysis. No receiver AGC was used. The recorded IF signals were played back through narrow bandpass filters which selected two components of the transmitted spectrum. Diode detectors extracted the envelope amplitudes which were then correlated (see figure 3). The correlation circuitry and procedure are described in the Appendix.

It is possible to obtain two estimates of the correlation coefficient simultaneously at the same frequency spacing by correlating the upper and lower sidebands with the carrier.

In comparing these simultaneous sideband carrier measurements approximately three-fourths differed by less than 20% or an absolute difference of less than 0.1. The data showed no preference for which sideband would produce the greater correlation with the carrier, and for analysis the two measurements were averaged.

A total of 56 observations was made and analyzed, 43 on 19 Mc/s and 13 on 14 Mc/s. In all but three cases the rhombic receiving antenna was used to obtain improved signal-to-noise ratios and reduce off-path interference. Observations were made on January 27 and 31, February 1, 2, 3, and 7, 1961, on 19 Mc/s and on February 17 and 24, 1961, on 14 Mc/s. Observations ranged from 3 to 15 minutes in duration and were made between the hours of 1130 and 1845 MST (105° West Time).

Figure 4 is a mass plot of all the data that were obtained. The simultaneous estimates of the correlation coefficient for frequency spacings of one and two times the modulating tone are joined together by a straight line. The modulating tone was varied on a prearranged schedule from 0.2 to 3.0 kc/s, which resulted in spacings from 0.2 to 6.0 kc/s. Unfortunately a very limited amount of data was obtained at the lowest frequency spacing.

It is readily apparent that the fading correlation bandwidth can vary appreciably. Median and upper and lower decile correlation curves based on figure 4 are shown in figure 5. The correlation bandwidth (correlation = 0.5) for the median curve is about 4 kc/s, while the value exceeded 90% of the time is 1 kc/s. It appears that the 10% value was considerably more than 6 kc/s.

The wide variation in bandwidth was investigated by subdividing the data according to different parameters. Parameters used were fading rate, time of day, magnetic activity, and the ratio of the operating frequency to the MUF. The subdivision could not be carried too far because of the limited amount of data. Although the effects of these parameters were examined separately, they are related. The MUF varies with time of day and is affected by magnetic activity while fading rate is a complex function of many factors.

To study the effects of fading the data were subdivided into groups of fast and slow fading, with 3 fades per second as the dividing line. Smaller subdivisions were tried but did not seem to yield any more information. As shown in figures 6 and 7 the median fading correlation bandwidth for fading rates of less than 3 c/s was 5 kc/s, while for fading rates greater than 3 c/s it was 3 kc/s. This indicates a possible dependence upon fading rate. Previous experience on this path had been that low fading rates are usually associated with magnetically quiet days and signals which frequently have periodic fading, indicating only two dominant coherent multipath components, while higher fading rates are usually associated with disturbed days and a more random type of fading, indicating the presence of scattering or turbulence in the ionosphere.

The difference between quiet and disturbed days can be seen by referring to figures 8 and 9. Figure 8 is for a quiet day with fading rates of less than 1 c/s during all the observations, while figure 9 is for a magnetically disturbed day with fading rates for all observations of about 7 or 8 c/s. Both sets of observations were at 14 Mc/s, the quiet-day observations being made between 1515 and 1845 MST and the disturbed-day observations between 1145 and 1500 MST, which in each case was the time of day providing the best signals. The quiet-day signals were 15 to 20 db stronger than the disturbed signals. A comparison of MUF's for the two days was impossible because excessive absorption on the northern half of the path prevented foF2 observations. Although there is hardly enough data in either case to draw a meaningful median curve, it is apparent that the bandwidth was greater on the quiet day.

The data were also examined for effects related to the time of day. Figure 10 contains median curves of correlation versus frequency spacing for various times of the day. Three of the periods are of one-hour duration while the earliest and latest were made somewhat longer in order to maintain about the same number of samples in each group. The median curves suffer from a degree of inaccuracy because of the limited data in each group, but they do indicate a trend. The fading correlation bandwidths have been tabulated in table 1. There appears to be a broad minimum about 1400 MST which corresponds to about 1300 at the path midpoint. This is not unexpected since at that time of day the MUF would be highest, resulting in greater multipath delay for fixed-frequency operation.

Table 1.

COMPARISON OF FADING CORRELATION BANDWIDTH WITH TIME OF DAY

Time of Day	Bandwidth
1100-1300 MST	4.75 kc/s
1300-1400	2.8 kc/s
1400-1500	2.8 kc/s
1500-1600	5.9 kc/s
1600-1845 MST	5.5 kc/s

It was intended to examine the effect of the ratio of operating frequency to the two-hop MUF, but insufficient information was available for a reasonable analysis. The MUF was to be determined by extrapolating the foF2 critical frequencies obtained from vertical soundings at Fairbanks, Alaska, and Boulder, Colorado, to the path reflection points and then applying the secant ϕ factor for oblique incidence. Excessive absorption and sporadic E on the northern half of the path prevented determination of MUF's on all but quiet afternoons.

Figure 11 contains all of the observations for which the MUF was determined. The number associated with each line is the ratio of operating frequency to the MUF. The median ratio was 0.87 which, using Salaman's [1962] MRF curves, indicates multipath differential delays on the order of 0.5 msec. Since the data included in figure 11 were obtained under conditions in which the multipath components would be well-defined, there should be a minimum in the correlation near 1 kc/s and a maximum near 2 kc/s. Although there is not much evidence of the minimum, mostly due to a lack of data, there is some indication of a maximum near 2 kc/s. The highest values of correlation appear in the proper area, and also the data segments with positive slope in the 1-kc/s to 2-kc/s area contribute to the appearance of a maximum near 2 kc/s. This corresponds to a plausible high-low ray multipath difference of about 0.5 msec.

About 20% of the observations resulted in data segments having a positive slope, with the great majority occurring on relatively quiet days (see figure 4). This is further support of the theoretical model described earlier.

In considering these results it is well to keep in mind that the correlation coefficients were obtained by averaging over periods ranging, in all but one case, from 5 to 15 minutes. The minute-to-minute variations can be quite large. Figure 12 contains a series of scatter diagrams made at one-minute intervals. The diagrams were made in the conventional manner by applying the envelope voltage of the upper sideband to the vertical deflection plates of an oscilloscope and the carrier envelope to the horizontal deflection plates. The frequency spacing between the two signals was one kc/s. The diagrams represent one-minute samples and were made consecutively. One could estimate the correlation directly from these diagrams [Sugar, 1954], but they were included here only to show how the correlation can change from minute to minute.

4. SHORT-TERM FREQUENCY PERTURBATIONS OF A HIGH-FREQUENCY CARRIER

Although modern technology has achieved very accurate control of the carrier frequency of HF transmitters, there are usually uncontrolled frequency variations in the received signal due to the vagaries of ionospheric propagation. These variations can be divided into long-term changes, i.e., durations of minutes or hours, due to diurnal changes in layer heights or electron densities and short-term changes, i.e., on the order of milliseconds, due to interference among the various multipath components.

Investigations of long-term changes [Fenwick and Villard, 1960; Watts and Davies, 1960] have shown frequency shifts as great as 5 or 6 cps. Such variations would be important in applications such as monitoring of standard broadcasts but probably would be inconsequential in FSK digital communications. The much larger short-term changes which would be important in communication system performance have been, for the most part, neglected. These changes are the subject of this part of the report.

4.1. Theoretical Curves

The variation in instantaneous frequency that results from the interference between two unmodulated carriers of approximately the same frequency has been described many times. Curves similar to those obtained by Cuccia [1952] which illustrate the variations of instantaneous frequency for several amplitude ratios of the interfering carriers are shown in figure 13.

One might use this description as the basis for a model of the HF signal, but it would be of limited value. Although the received signal may frequently contain only two multipath components and, therefore, fit the preceding description, the amplitude ratio will vary widely as the two components fade independently. The frequency difference will also be subject to random variations. As a result the model chosen for comparison with the observations should be of a random nature. This would be especially true when the received signal contains many multipath components.

In view of this and the fact that the amplitude statistics of an HF signal are frequently approximated by Rayleigh distributions, a model based on narrow-band Gaussian noise seems appropriate. Some statistics for the instantaneous frequency of such a model have already been obtained [CCIR, 1959]. In this case, for simplicity, a rectangular noise spectrum was assumed, although a Gaussian-shaped spectrum would probably be a more accurate representation. The theoretical distribution of deviations from the average frequency are given in figure 14. The frequency deviation has been normalized with reference to the fading rate, the fading rate being 1/2.32 times the width of the rectangular noise spectrum.

Cumulative distributions alone are not sufficiently revealing; information is also needed about the duration of the frequency excursions. Theoretical distributions containing this information are not available, but measured distributions were obtained. The aforementioned CCIR report does give average duration of the frequency excursions as a function of frequency deviation.

4.2. Experimental Results

Observations of the instantaneous carrier frequency were made over the same path and with the same transmitting and receiving equipment as the correlation measurements (see figure 2). Data were obtained on both 14.688 Mc/s and 19.247 Mc/s from August 9, 1961 to August 22, 1961, using both dipole and rhombic receiving antennas.

Figure 15 is a block diagram of the frequency-detection equipment. The 10-kc/s IF signal from the receiver was amplitude-limited and then fed to a frequency discriminator. The discriminator produced a pulse of constant amplitude and width with the leading edge coincident with the positive-going zero-crossings of the input signal. The result was pulse train whose average d-c level was proportional to the input frequency. In this situation the 10-kc/s and higher frequency components arising from the pulse repetition rate were removed by filtering, leaving approximately 10 volts d-c corresponding to the 10-kc/s input frequency. The average d-c level was subtracted by the series d-c supply, leaving voltage variations corresponding to the frequency deviations from the average carrier frequency. At the output of the discriminator the scale factor was 1 mv/cycle.

Equipment noise was sufficiently low to permit observation of frequency changes of less than one c/s. Unfortunately this was not always true when actual signals were being observed, the received signal-to-noise ratio frequently being such as to mask the smaller frequency changes. In addition, the large frequency changes were usually accompanied by fading of the carrier which resulted in additional noise degradation of the signal. To alleviate this condition during data reduction, the post-detection bandwidth was reduced to 75 c/s by adding a low-pass filter between the tape-playback equipment and the analysis equipment. Figure 16a illustrates the improvement obtained by addition of the filter. The cut-off frequency chosen did not seem to have a serious effect on the desired data. This bandwidth was also comparable to the post-detection bandwidth in single-channel FSK systems. Figure 16b depicts some of the frequency perturbations that were observed. Note that the frequency changes appear in both directions and are coincident with fades in envelope amplitude. This was typical of signals with low fade rates, and was similar to the situation of two interfering carriers described earlier (figure 13). Figure 16c illustrates the more random variations found at higher fade rates.

The equipment used for data reduction was essentially the same as that used previously for analysis of fading on this path [Koch, Beery, and Petrie, 1960] . Cumulative distributions of frequency deviation from the average frequency were obtained as were distributions of frequency deviation exceeded for various durations from 1.0 to 100 or 250 milliseconds.

All distributions were based on a 200-second sample length. The curves are presented as averages of the deviation on each side of the carrier. This results in the distribution being asymptotic to the 50% line as the deviation approaches zero.

The cumulative distributions followed the general shape of the theoretical curve. Examples for a variety of fade rates are given in figures 17, 18, and 19. A comparison with the narrow-band noise model was made by translating the measured curves to the left or right to bring them into coincidence with the theoretical curve. Because of the logarithmic frequency scale, this was equivalent to dividing the frequency excursions indicated by the curve by a normalizing factor. Obviously, exact coincidence is not obtained unless the curves have identical shapes. The agreement between curve shapes ranged from "good" to "poor" as shown in figure 20. If, because of curve shape, there was some question as to the exact normalizing factor, coincidence of the right-hand portions of the curves was weighted most heavily, since this is the area of interest from the standpoint of FSK telegraph errors.

The normalizing factor obtained in this manner is plotted versus fade rate in figure 21. A straight line having a reasonable fit to these points has a slope of 1.4. This is to say, on the average, frequency deviations occurred with probabilities given by the theoretical curve, if 1.4 times the fade rate is used in place of the fade rate for the normalizing factor.

It should be realized that this factor was obtained from a limited number of observations on a particular path and may be different for other situations.

A factor closer to unity might have been obtained if the model had used a Gaussian-shaped noise spectrum instead of a rectangular-shaped spectrum. The long "tails" on the Gaussian-shaped spectrum would have contributed to more violent frequency excursions and might have made the theoretical distribution more directly comparable to the observed distributions.

Cumulative distributions of frequency deviation do not give any insight into the duration of individual frequency excursions. For this type of information one is referred to figures 22 through 29. These figures are families of curves giving the per cent of time that the frequency excursions exceed a given magnitude for periods greater than a given duration. Each figure contains a family of curves obtained from the same data sample with duration as the parameter. The figures given are typical of the data that were obtained. Figure 23 illustrates the smallest frequency deviations observed,while the largest deviations are given by figure 29 for durations up to 25 msec and by figures 27 and 28 for durations of 50 and 100 msec respectively.

Unfortunately, similar distributions are not available for the theoretical model. The CCIR report mentioned earlier does contain curves of the average duration of frequency deviations exceeding particular values. The data reduction methods used did not permit comparison with this information.

5. CONCLUSIONS

Measurements of the correlation between the fading envelopes of HF carriers at frequency spacings from 0.2 to 6.0 kc/s indicated a mean fading correlation bandwidth of 4.3 kc/s. The bandwidth that was exceeded 90% of the time was 1.0 kc/s. The upper decile value was not obtained because it exceeded the largest spacings observed.

The effect of fading rate and magnetic activity was investigated. The fading correlation bandwidth was found to decrease with increased magnetic activity and with increased fade rate.

The effect of time of day was also investigated,and a broad minimum in correlation bandwidth was found about midday. This minimum coincides with the minimum in the ratio of the observed carrier frequency to the lowest order (two-hop) MUF. At this time high-low ray differential multipath delays would be the greatest, indicating a general agreement with what was suggested by the rather elementary model described earlier, i.e., that the fading correlation bandwidth is inversely proportional to the multipath delay.

A lack of detailed propagation information prevented a more detailed examination of the relationship between correlation bandwidth and the ratio of the operating frequency to the MUF. There is some evidence, however, that the correlation versus frequency spacing function contains an oscillatory component whose period is the reciprical of the delay time, as was suggested by the simplified model.

It is suggested that future correlation measurements be made concurrently at several frequency spacings to provide more detailed information as to the nature of the correlation versus frequency spacing function. Simultaneous sweep-frequency pulse transmissions over the same path would be invaluable in determining what propagation modes were present, and would allow one to relate the bandwidth measurements to the propagation characteristics. Such information would permit some degree of prediction of bandwidth in the future, on the same or other paths.

Statistical distributions were obtained of the frequency deviation of an HF signal from its average carrier frequency. These distributions were compared with a theoretical distribution based on a narrowband noise model. Reasonable agreement was obtained if a normalizing factor of 1.4 times the fade rate was used rather than the fade rate.

Distributions were also obtained which indicate the duration of the frequency deviations. These were not compared with theoretical distributions. The results do indicate that frequency deviations of this nature would not be a significant source of errors in FSK digital communications for the frequency shifts and baud rates commonly used, i.e., for shifts of greater than 100 c/s, and element lengths greater than 10 or 15 msec.

Because frequency deviations were found to be closely related to fading rate and only indirectly to other propagation parameters, and because of the difficulty of precise mode determination without simultaneous sweep frequency recordings, comparisons of frequency deviations with factors other than fade rate were not attempted.

6. ACKNOWLEDGEMENTS

The logistical support and other assistance provided by the Arctic Research Laboratory, Barrow, Alaska, Max Brewer, Director, was invaluable and greatly appreciated.

The author also appreciates the assistance of J. L. Workman (Barrow, Alaska), G. E. Wasson, E. L. Komarek, and C. H. Johnson in obtaining and analyzing the data and the advice and comments of R. K. Salaman on propagation problems. The author also acknowledges the work of J. W. Koch in originating the project.

7. REFERENCES

Bell, J., Correlation between fading signals, Electronic Technology 23, 36-40 (Jan. 1960).

C.C.I.R., Influence on long-distance high-frequency communications using frequency shift keying of frequency changes due to passage through the ionosphere, Report No. 111, IXth Plenary Assembly, Los Angeles 3, 89 (1959).

Cuccia, C. L., Harmonics, sidebands and transients in communication engineering, 287-289 (McGraw Hill, New York, N.Y., 1952).

Davenport, W. B., Jr., R. A. Johnson, and D. Middleton, Statistical errors in measurements on random time functions, J. Appl. Physics 23, 377-388 (April 1952).

Fenwick, R. C., and O. G. Villard Jr., Continuous recordings of the frequency variation of the WWV-20 signal after propagation over a 4000 km path, J. Geophys. Research 65, 3249-3260 (Oct. 1960).

Koch, J. W., Factors affecting modulation techniques for VHF scatter systems, IRE Trans. of PGCS CS-7, 77-92 (June 1959).

Koch, J. W., and H. E. Petrie, Fading characteristics observed on a high-frequency auroral radio path, NBS Jour. of Res. 66D, 159-166 (Mar. - Apr. 1962).

Koch, J. W., and W. M. Beery, Observations of radio wave phase characteristics on a high-frequency auroral path, NBS Jour. of Res. 66D, 291-296 (May-June 1962).

Meyers, K. A., and H. B. Davis, Triangular-wave analog multiplier, Electronics 29, 182-186 (August 1956).

Norsworthy, K. H., A simple electronic multiplier, Electronic Engineering 26, 72-76 (Feb. 1954).

Salaman, R. K., A new ionospheric multipath reduction factor (MRF) IRE Trans. of PGCS CS-10, 220-222 (June 1962).

Staras, H., Diversity reception with correlated signals, J. Appl. Physics 27, 93-94 (Jan. 1956).

Staras, H., Tropospheric scatter propagation - a summary of recent progress, RCA Review 19, 3-18 (March 1958).

Sugar, G. R., Estimation of correlation coefficients from scatter diagrams, J. Appl. Physics 25, 354-357 (March 1954).

Watts, J. M., and K. Davies, Rapid frequency analysis of fading radio signals, J. Geophys. Research 65, 2295-2303 (August 1960).

8. APPENDIX

Instrumentation to determine correlation coefficients was considerably simplified by adopting an approximation given by Bell [1960]; that is,

$$\rho = \frac{\overline{xy}}{\left(\overline{x^2}\,\overline{y^2}\right)^{\frac{1}{2}}} \approx \frac{\overline{2xy}}{\overline{x^2+y^2}}, \tag{1}$$

where ρ is the normalized correlation coefficient and x and y are the zero mean time varying functions to be correlated. This approximation introduces less than 1% error if the variances of x and y are within 40% of each other. The form of the instrumentation follows readily from this equation. The sum and difference of the input functions are formed and then squared. Then the sum and the difference of these squared quantities are formed, the difference yielding the numerator, the sum yielding the denominator; that is,

$$(x + y)^2 - (x - y)^2 = 4\,xy \tag{2}$$

and

$$(x + y)^2 + (x - y)^2 = 2\,(x^2 + y^2). \tag{3}$$

Thus the circuitry has to perform addition, subtraction, squaring, and division. The most difficult, division, was performed by hand as one of the final operations. The other operations were easily performed with operational amplifiers using the triangular carrier-wave method to obtain the squaring capability [Norsworthy, 1954; Meyers and Davis, 1956].

The square-law characteristic is due to the area of similar triangles being proportional to the square of their heights. If a triangular wave of zero mean and peak amplitude V is full-wave rectified, the average value is $\frac{1}{2}V$. If to the triangular wave is added a signal s, which varies slowly compared to the triangular wave frequency, the average rectified output will be $\frac{1}{2}(V + s^2)$.

Figure 30 is a diagram of the correlator. The triangular blocks represent operational amplifiers, while the numbers adjacent to the input and feedback resistors indicate relative values. Amplifier 1 provides a sign reversal for the Y input,while amplifiers 2 and 3 are adders to form the sum and difference of the two inputs. Amplifiers 4, 5,and 8 are phase inverters to drive the full-wave diode rectifiers. Germanium diodes were used because of their low forward voltage drop. The only other requirement on the diodes is a sufficiently high inverse voltage rating, since peak voltages were as high as 100 V. Amplifiers 6 and 7 are combined adders and integrators, integrating with a 10-second time constant.

In unit 6, the squared terms and the constant due to the triangular carrier wave cancel, leaving the cross product average, while in unit 7 the cross products cancel, leaving the sum of the squares in the output, the carrier-wave constant being removed by adding in a similar constant of proper sign from amplifier 8.

One percent resistors were used for input and feedback elements. Some minor gain adjustments were made at the input to the integrator units to assure cancellation of the undesired input terms.

The outputs of units 6 and 7 were recorded on strip charts, one-minute averages taken,and the quotients formed manually. This resulted in a curve of correlation coefficient versus time, which was again averaged to obtain a single value for each run.

By definition the correlation coefficient implies averaging over infinite time. The loss of accuracy due to finite averaging time has been discussed at length elsewhere [Davenport, Johnson, and Middleton, 1952].

Multiple averaging as performed here is a method of avoiding some of the errors due to finite averaging time. Bell [1960] indicates that for applications such as this the observation period should be at least 100 times the interval between fades in order to obtain results significant at the 95% level for correlation coefficients on the order of 0.2. The observation times used in this experiment more than met this criterion.

This instrumentation scheme assumes that the input signals have zero means. This was accomplished by using long time constant RC coupling circuits. To eliminate the error that would be introduced by the charging of the coupling capacitors at the beginning of a run, provision was made for shorting out a large portion of the coupling circuit resistance in order to rapidly charge the coupling capacitor to approximately the mean value. An alternative was to make a preliminary run to charge the coupling capacitors and then play back the data again to obtain the correlation coefficient. This was especially useful on short runs where one could not afford to discard the initial portion of the run.

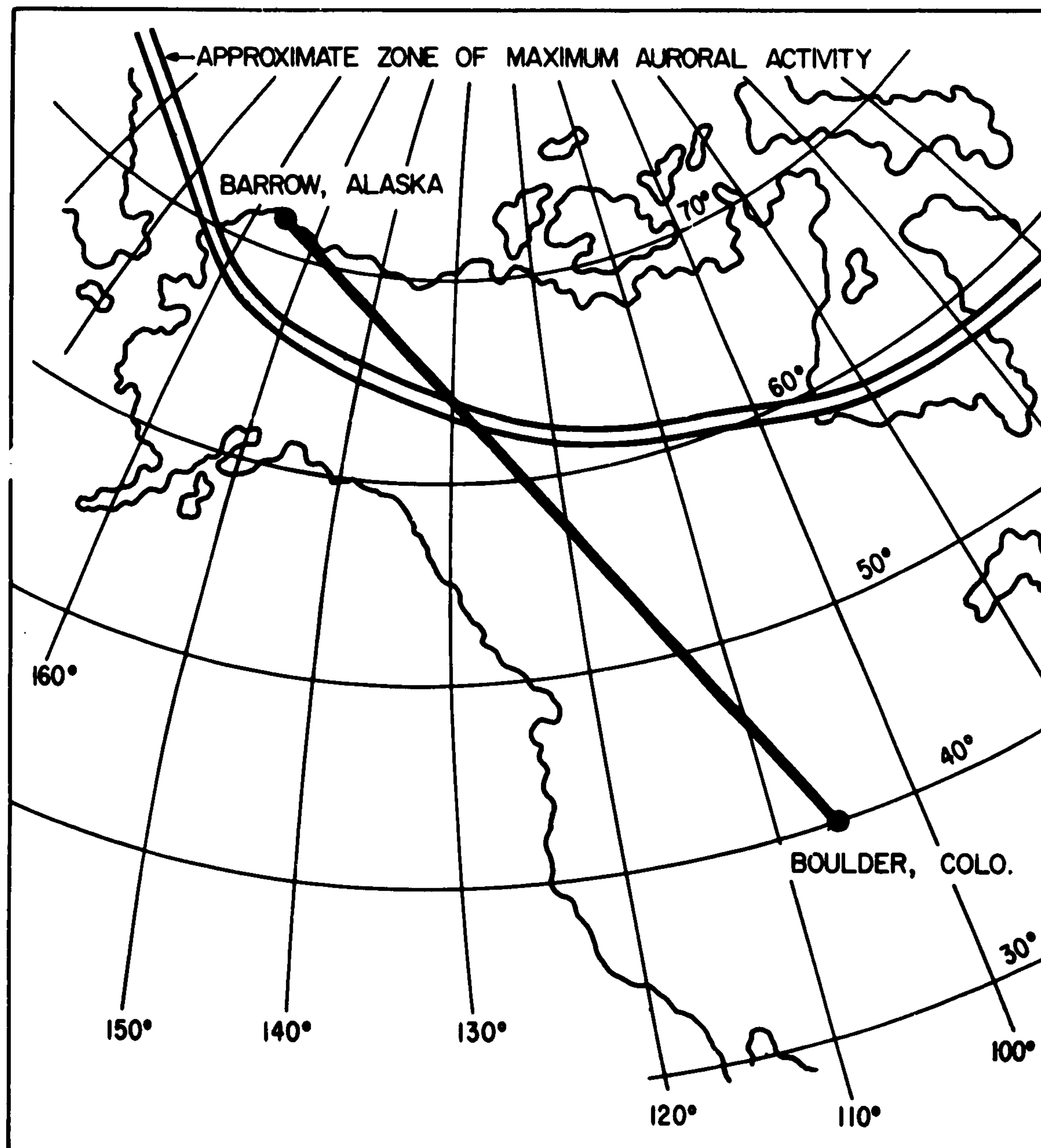

Figure 1. Geographic locations of the transmitter and receiver stations.

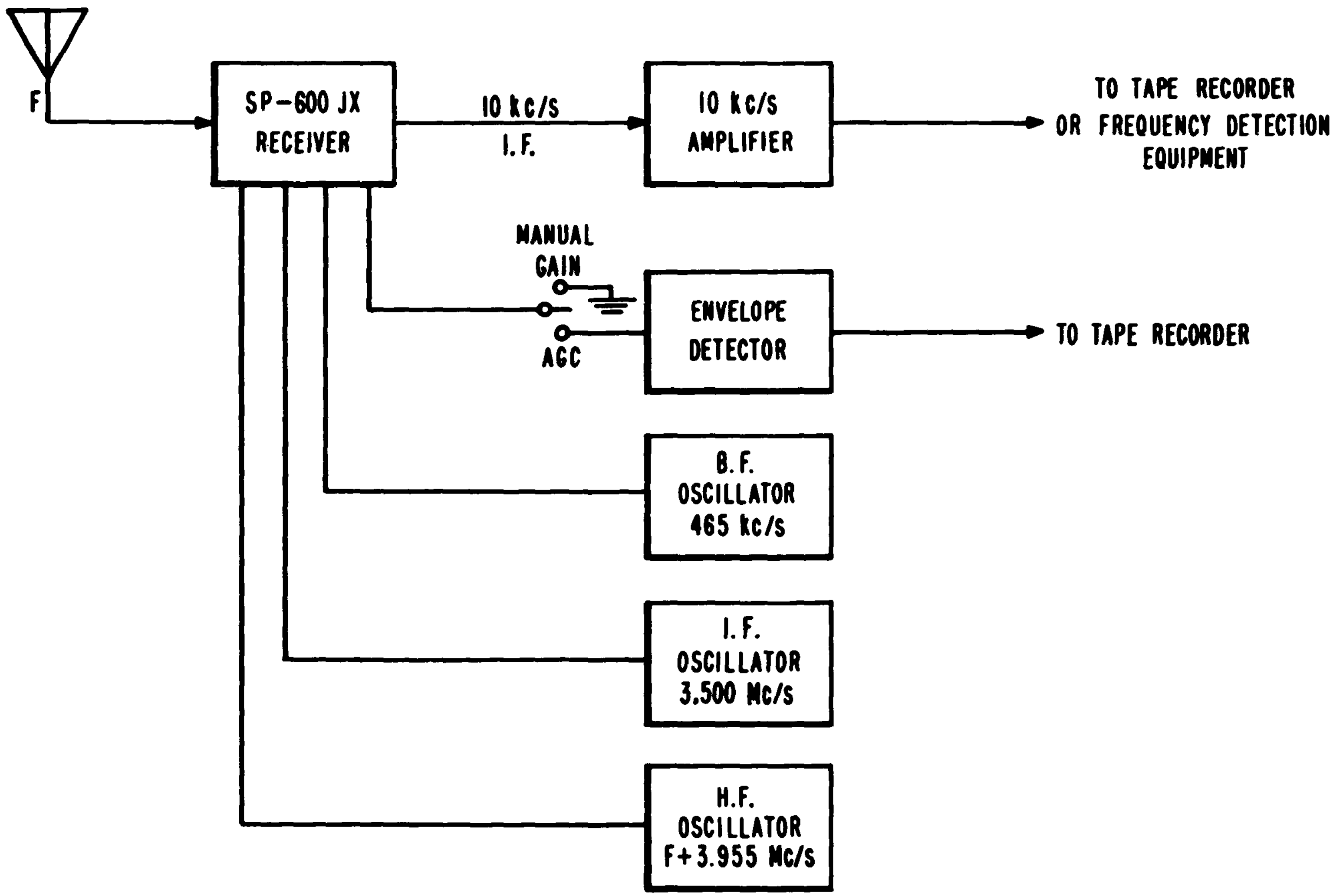

Figure 2. Block diagram of receiving equipment

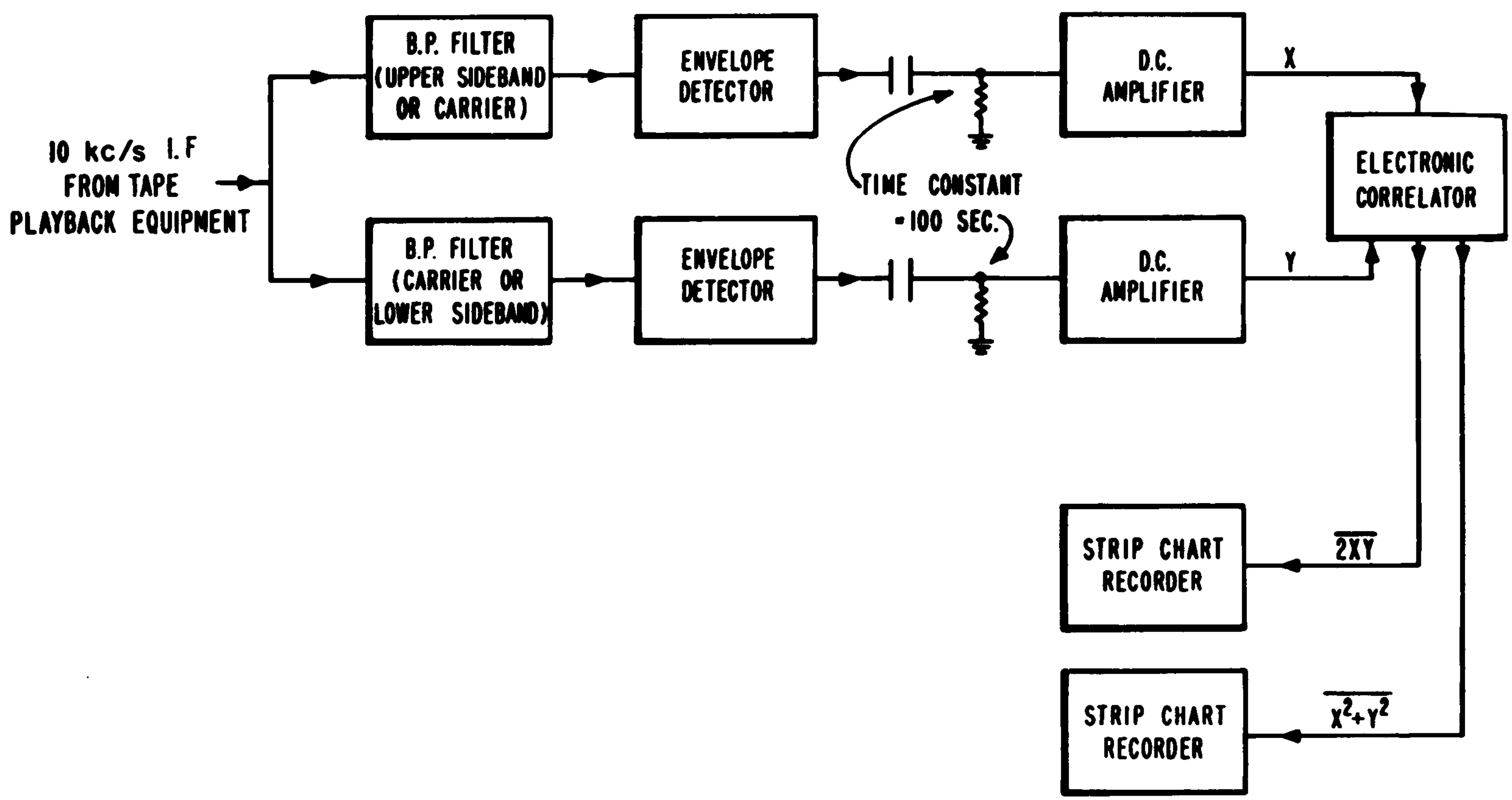

Figure 3. Block diagram of correlation measuring equipment

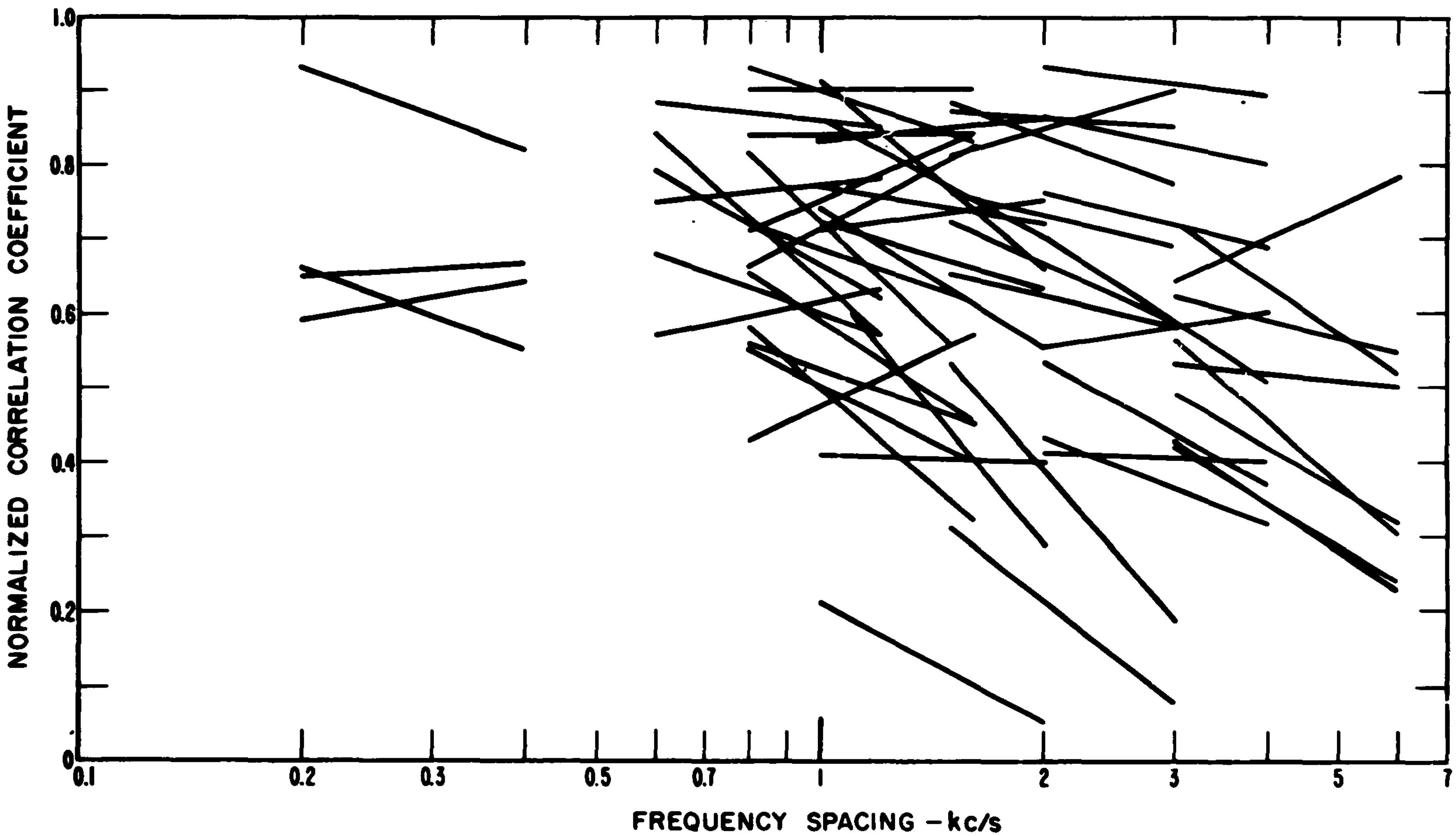

Figure 4. Mass plot of all correlation measurements

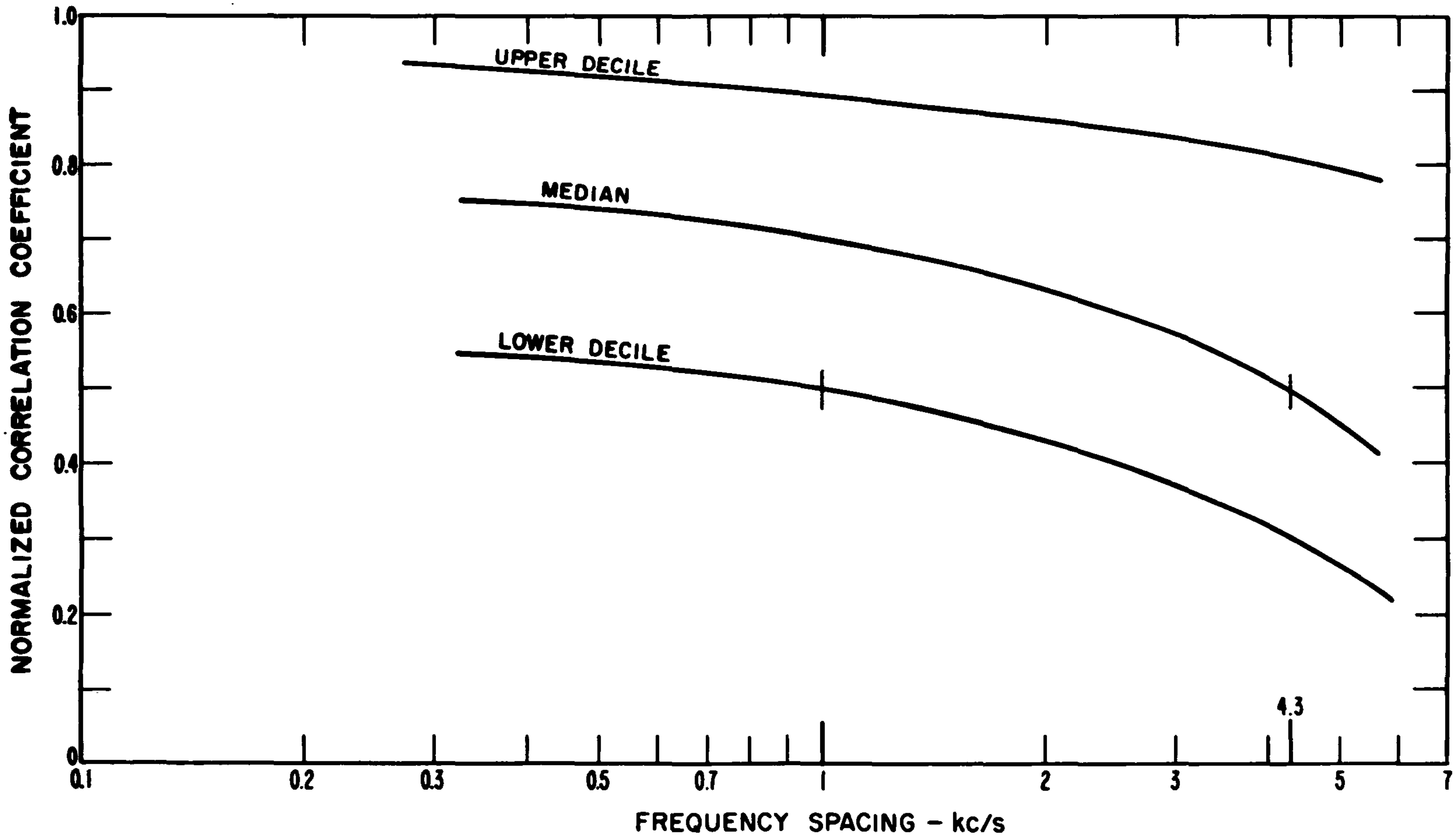

Figure 5. Median and upper and lower decile curves of correlation vs. frequency spacing

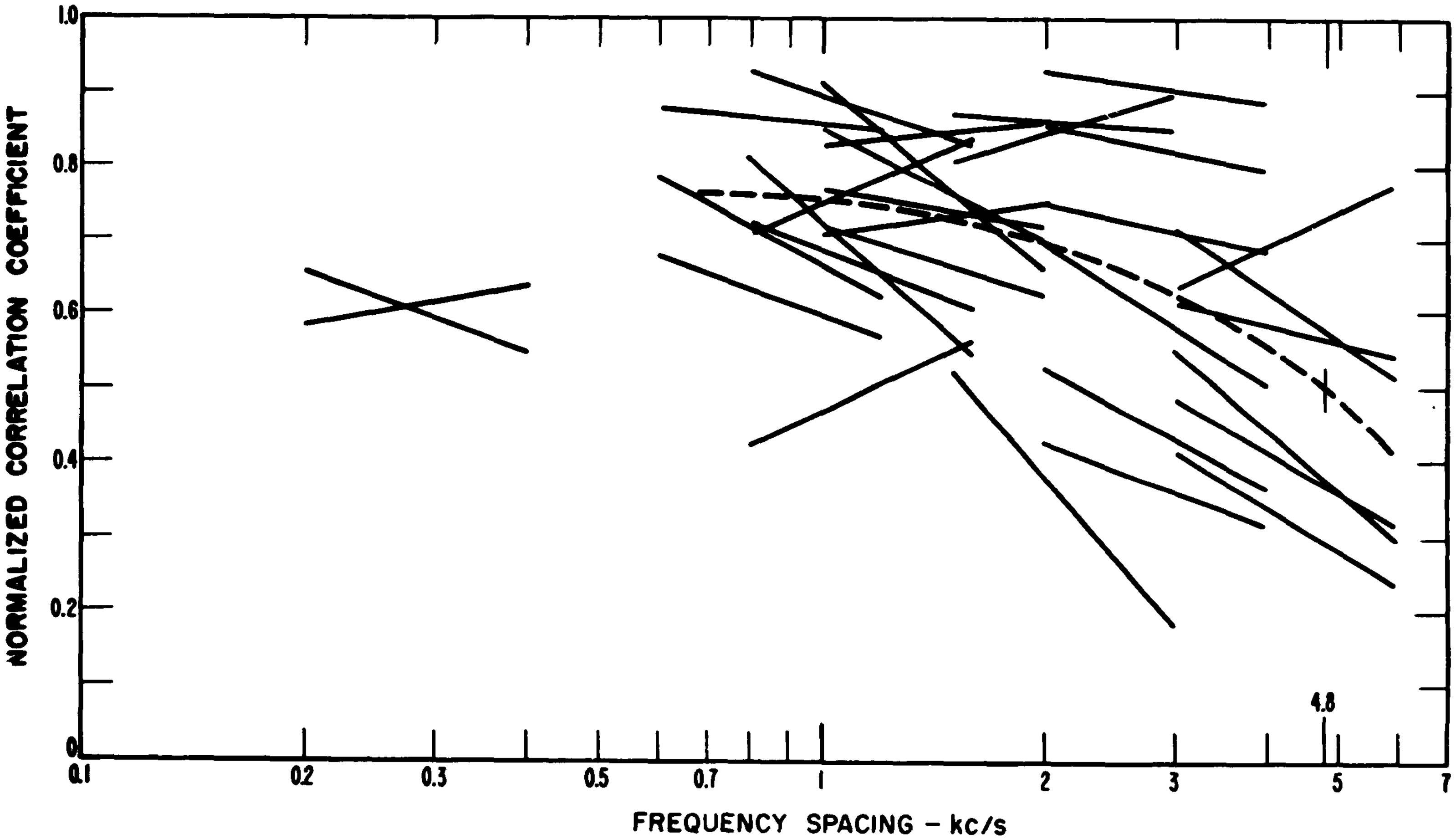

Figure 6. Correlation measurements for fade rates of less than 3 cps. The median correlation curve and correlation bandwidth are also indicated.

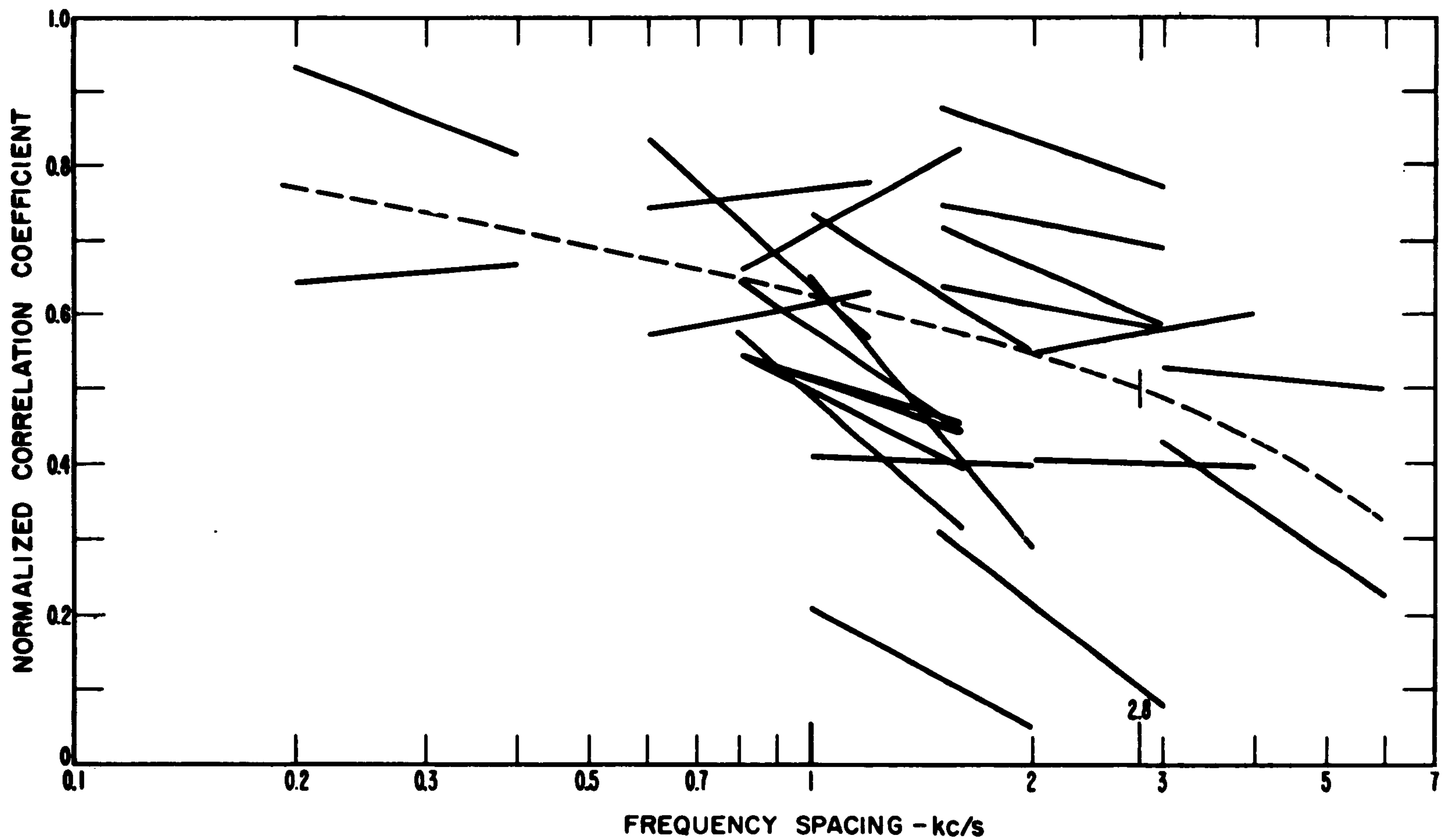

Figure 7. Correlation measurements for fade rates greater than 3 cps. The median correlation curve and correlation bandwidth are also indicated.

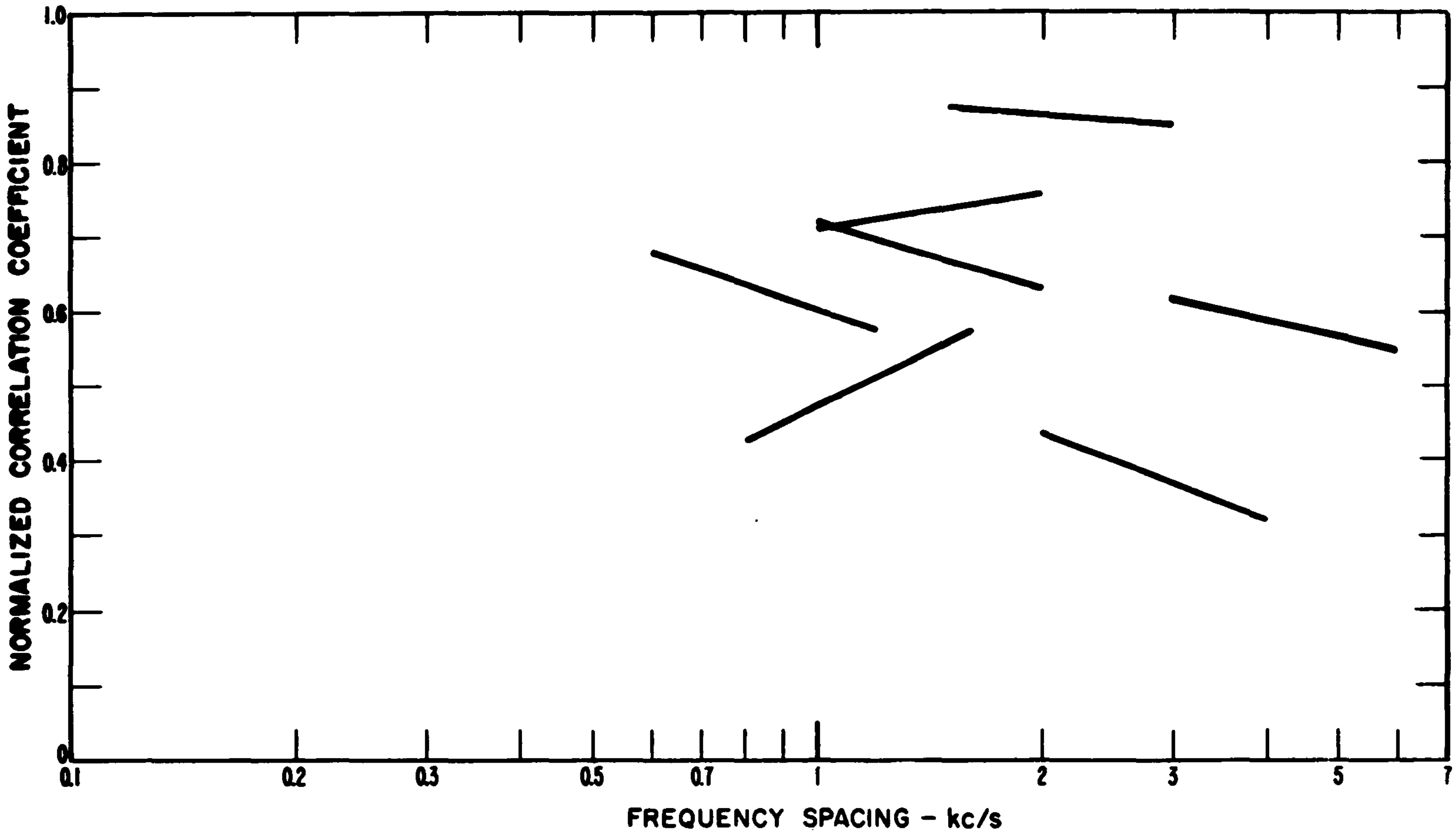

Figure 8. Correlation measurements made on a magnetically quiet day

Date: Feb. 24, 1961
Frequency: 14.688 Mc/s
Magnetic activity (K_p sum): 14-

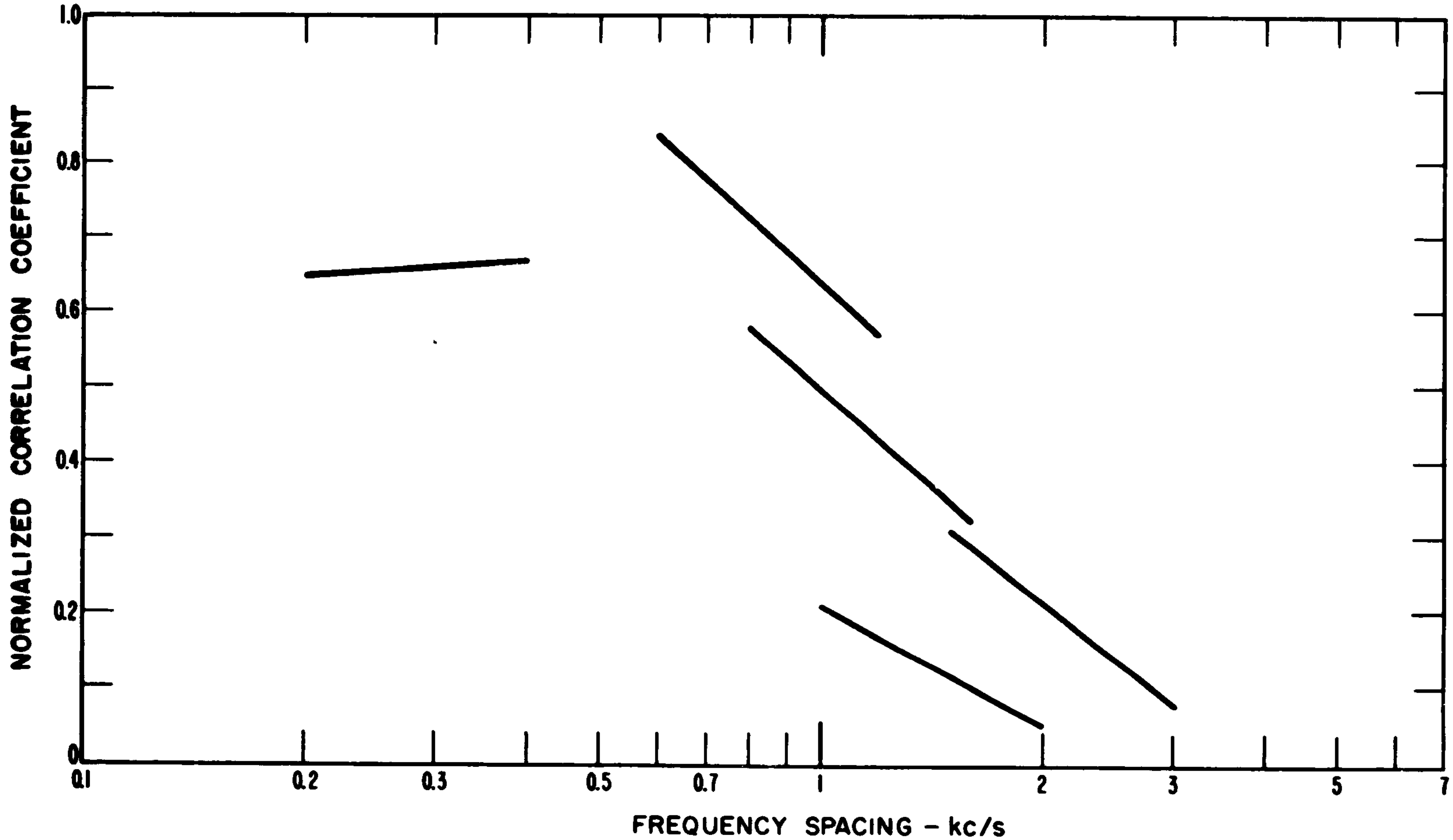

Figure 9. Correlation measurements made on a magnetically disturbed day

Date: February 17, 1961
Frequency: 14.688 Mc/s
Magnetic activity (K_p sum): 28-

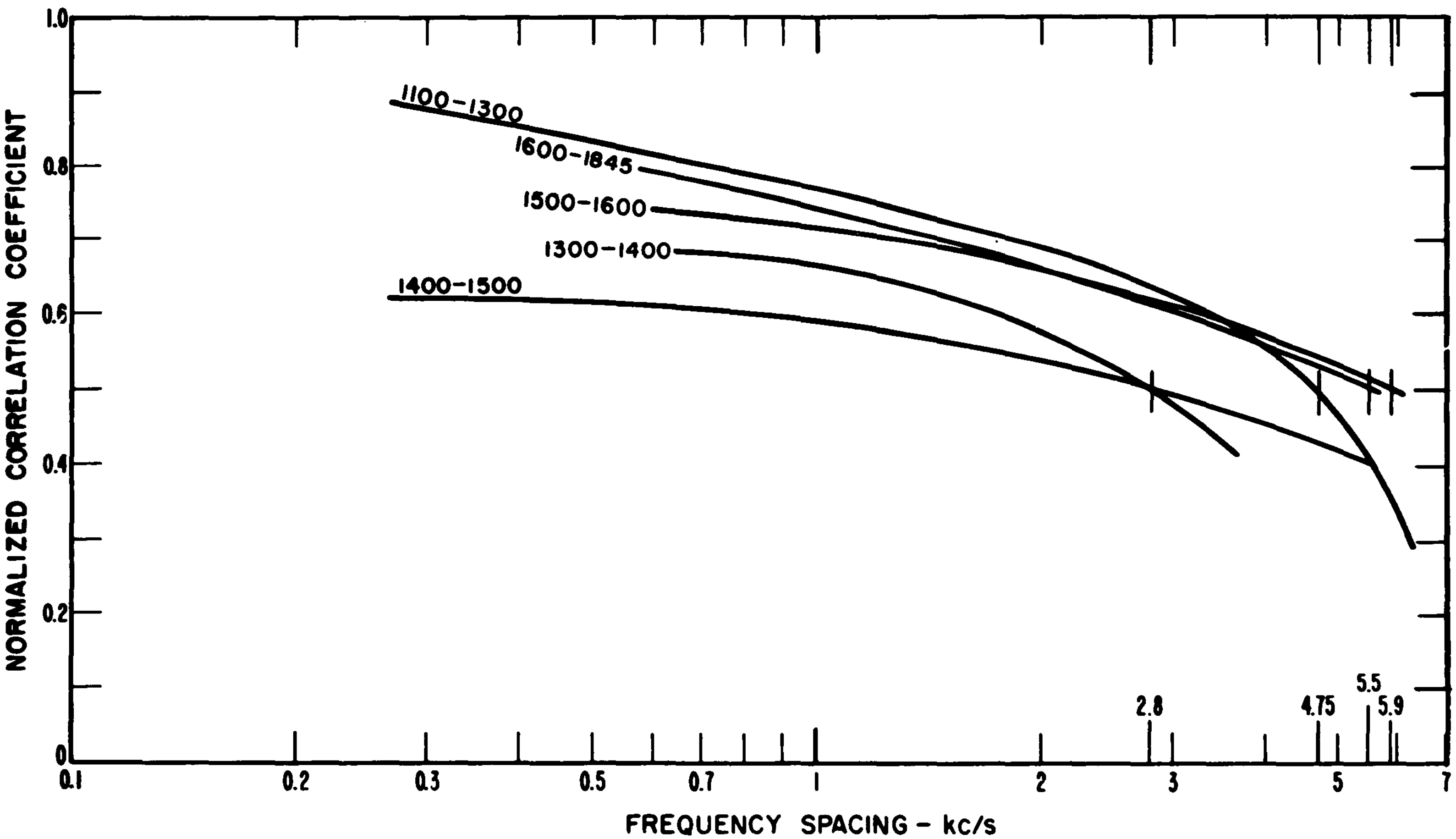

Figure 10. Median curves of correlation vs. frequency spacing for various times-of-day (MST). The fading correlation bandwidth is also indicated.

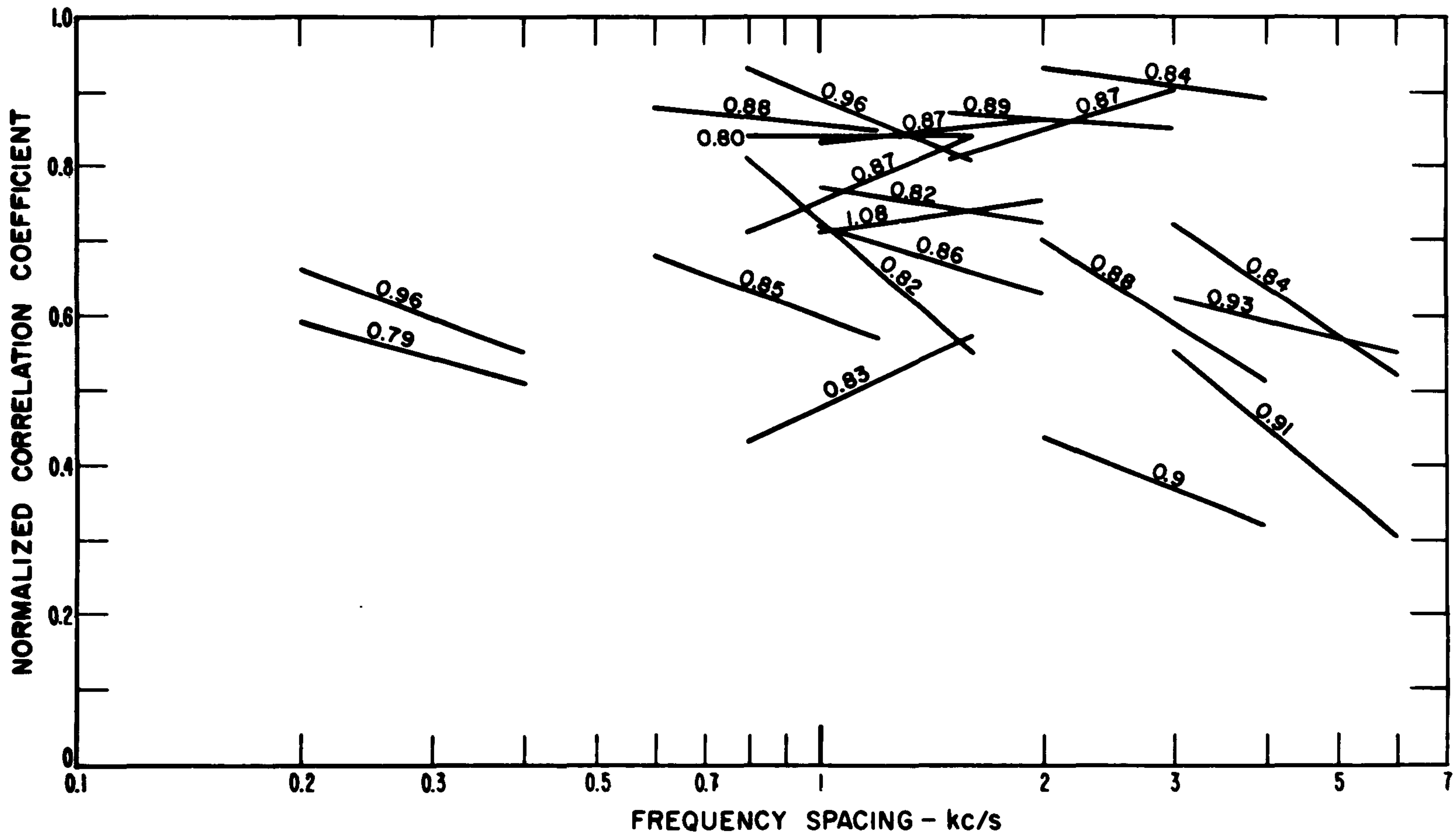

Figure 11. Correlation measurements for which the MUF could be determined. The number adjacent to each line is the ratio of the carrier frequency to the MUF.

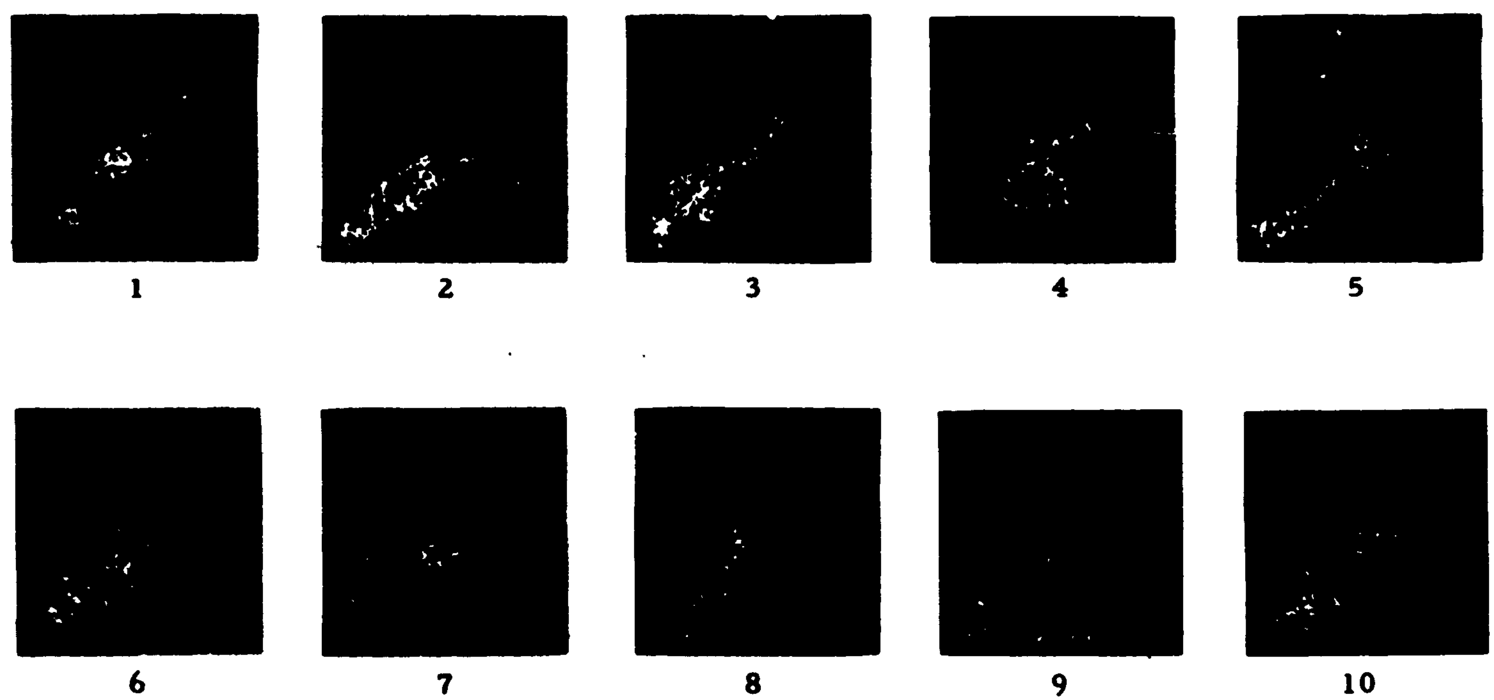

Figure 12. Scatter diagrams illustrating the variability in the correlation between two HF carriers spaced one kc/s The diagrams are consecutive one-minute samples.

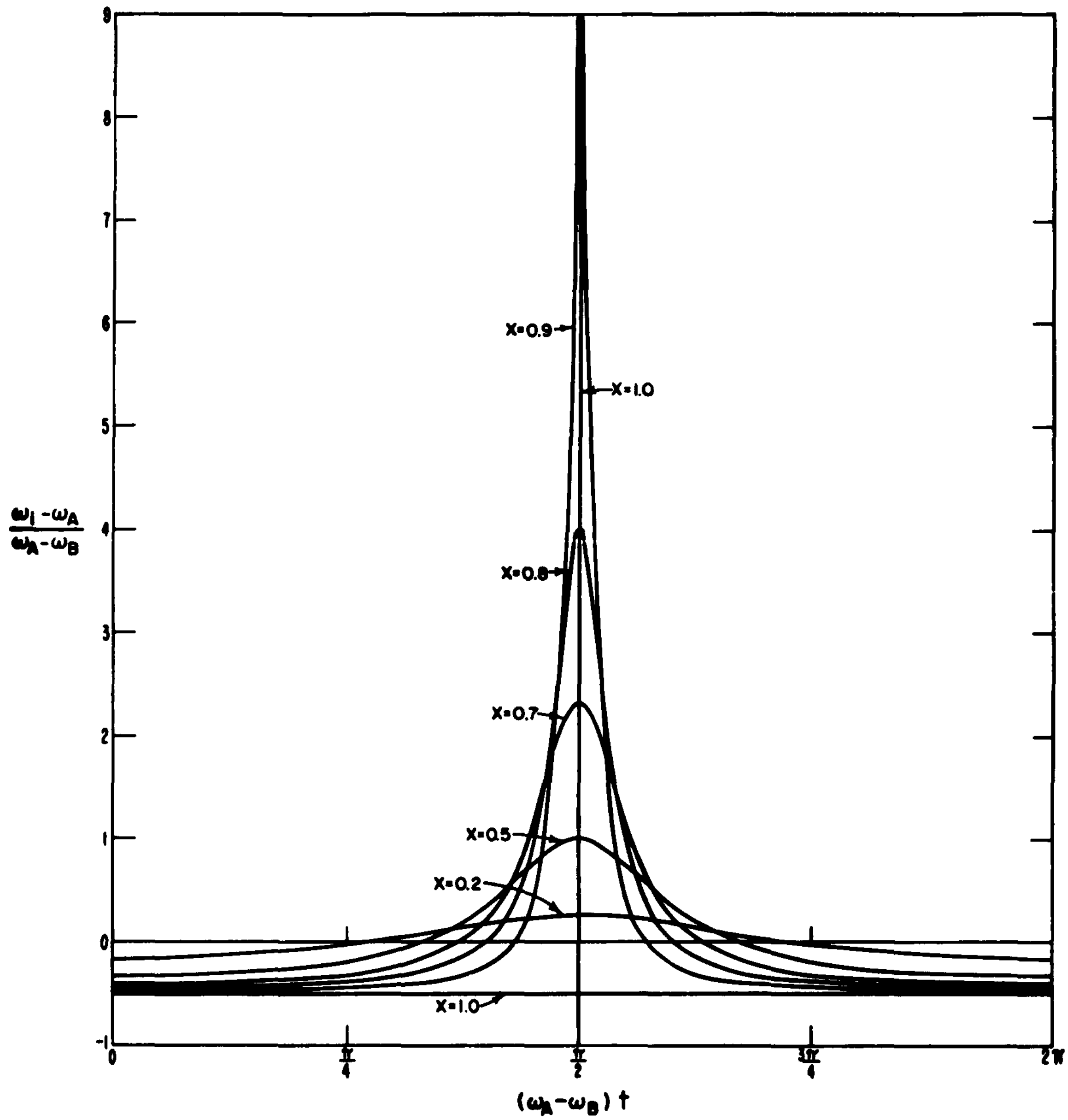

Figure 13. Deviation of the instantaneous frequency (ω_i) about the stronger (ω_A) of the two interfering carriers (ω_A and ω_B) The deviation is given in units of the frequency difference between the two carriers for various values of the ratio (x) of the amplitudes of the carriers. (after Cuccia)

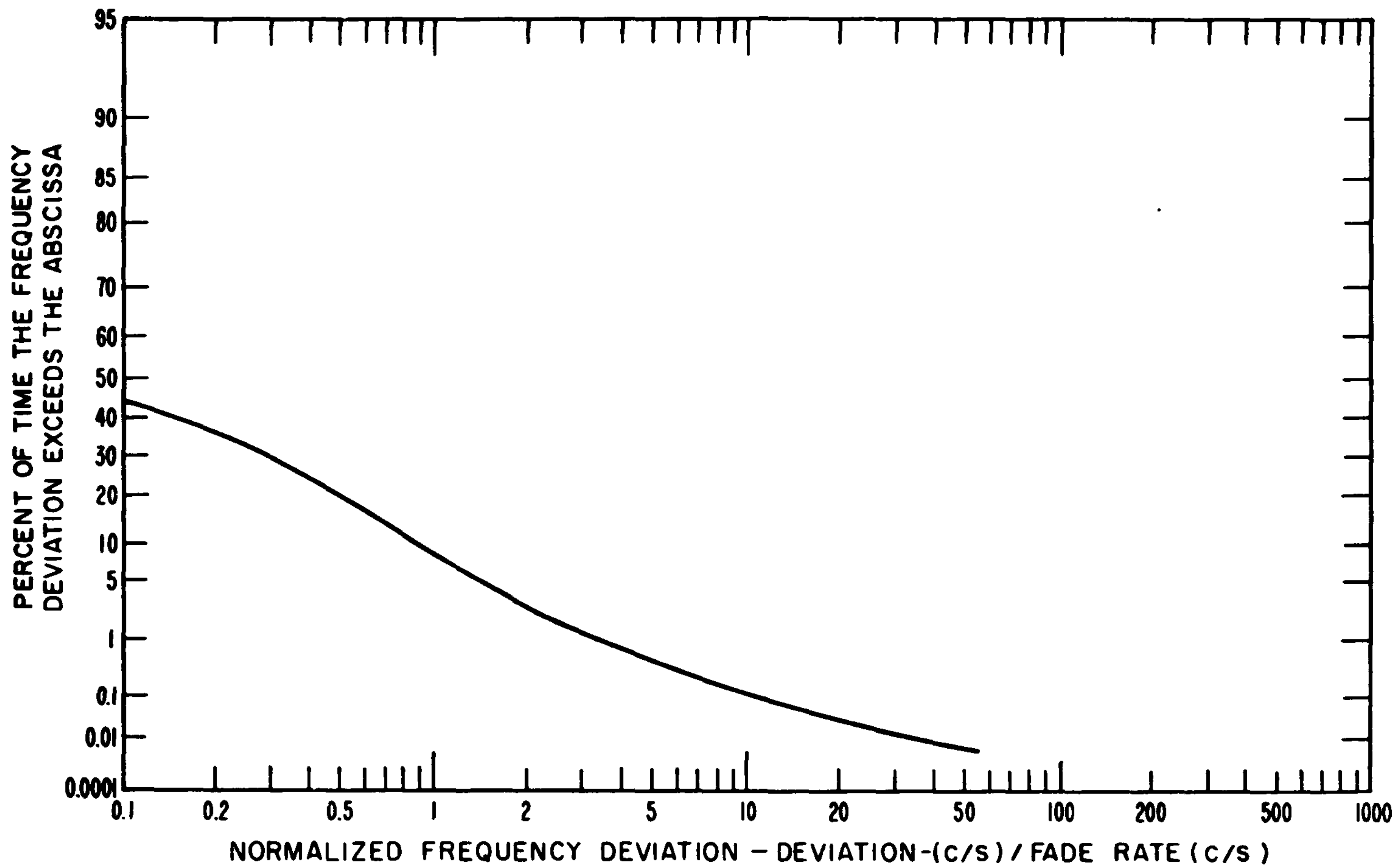

Figure 14. Cumulative distribution of the deviation of the instantaneous frequency from the average frequency of narrow band Gaussian noise (After CCIR, 1959)

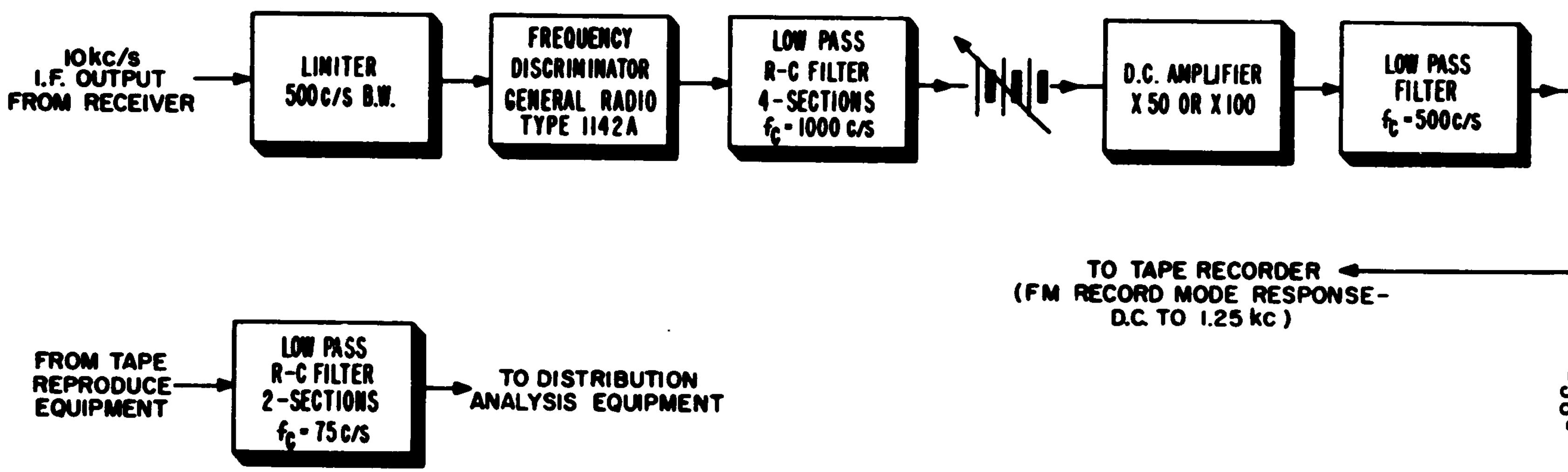

Figure 15. Block diagram of the frequency detection equipment

(a)

(b)

(c)

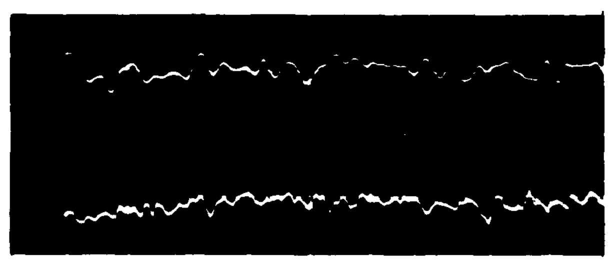

Figure 16. Illustrations of observed frequency deviations

(a) Effect of 75 cps low-pass filter on output
Upper trace - with filter; Lower trace - without filter
Time base 0.2 sec/div.; Vertical scale 20 cps/div.

(b) Frequency deviation (upper trace) and envelope voltage (lower trace) for an average fade rate of 1 cps
Time base 0.2 sec/div.; Vertical scale 20 cps/div.
Envelope voltage uncalibrated

(c) Frequency deviation (upper trace) and envelope voltage (lower trace) for an average fade rate of 4 cps
Time base 0.25 sec/div.; Vertical scale 20 cps/div.
Envelope voltage uncalibrated

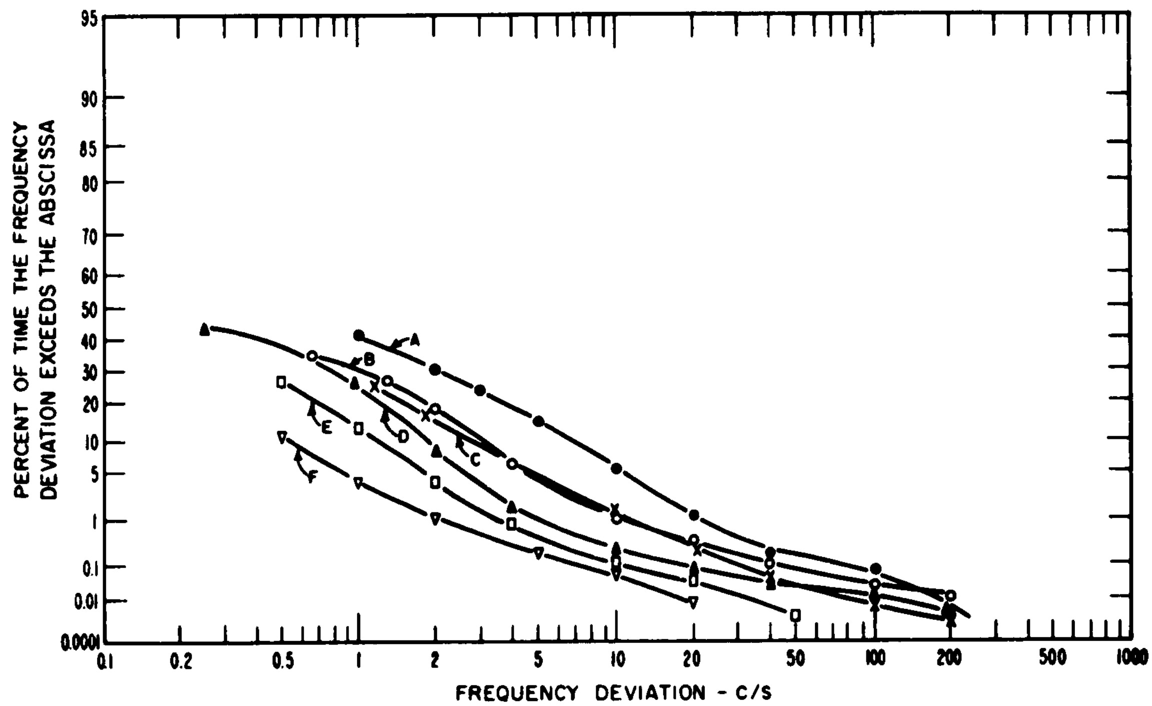

Figure 17. Cumulative distributions of frequency aeviations

A 14.688 Mc/s; August 8, 1961; 1000 MST; Fade rate 5 cps; S/N 25 db; Rhombic antenna

B 14.688 Mc/s; August 11, 1961; 2138 MST; Fade rate 1.5 cps; S/N 22 db; Rhombic antenna

C 14.688 Mc/s; August 11, 1961, 2120 MST; Fade rate 2 cps; S/N 31 db; Dipole antenna

D 19.247 Mc/s; August 15, 1962; 1229 MST; Fade rate < 1 cps; S/N 31 db; Dipole antenna

E 19.247 Mc/s; August 9, 1961; 1258 MST; Fade rate 1 cps; S/N 42 db; Rhombic antenna

F 14.688 Mc/s; August 9, 1961; 1921 MST; Fade rate 1 cps; S/N 40 db; Rhombic antenna

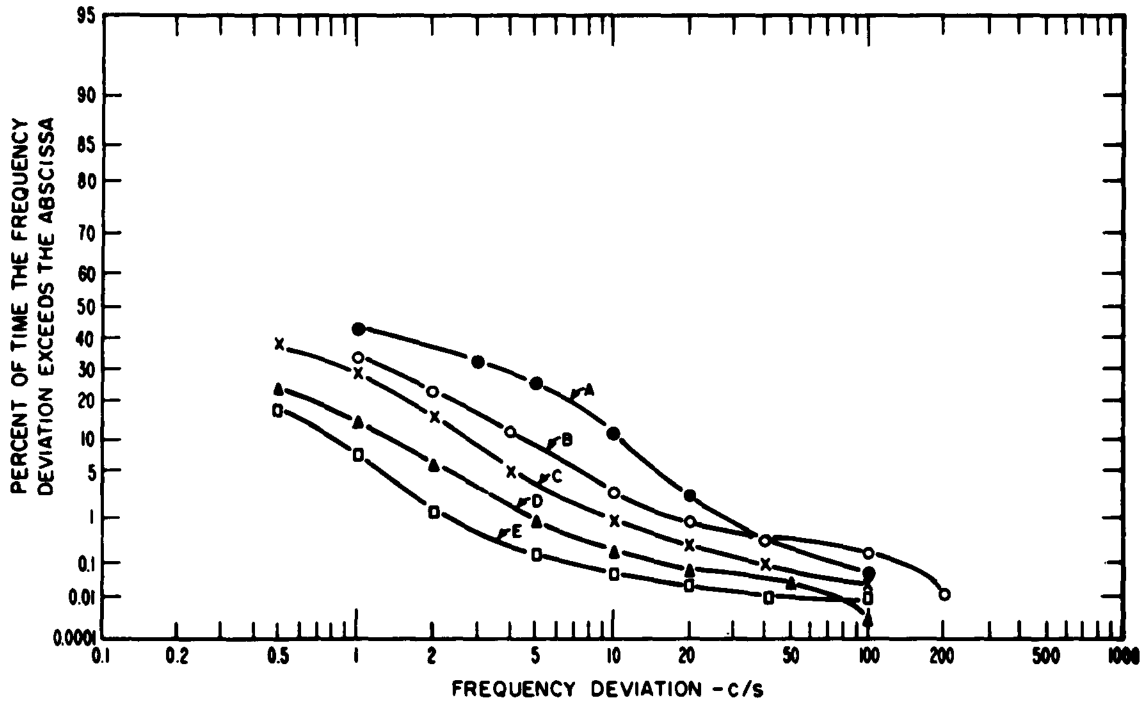

Figure 18. Cumulative distributions of frequency deviations

A 14.688 Mc/s; August 9, 1961; 2100 MST;
Fade rate 7 cps; S/N 24 db; Dipole antenna

B 19.247 Mc/s; August 9, 1961; 1954 MST;
Fade rate 4 cps; S/N 22 db; Dipole antenna

C 19.247 Mc/s; August 21, 1961; 0747 MST;
Fade rate 1.25 cps; S/N 27 db; Rhombic antenna

D 14.688 Mc/s; August 15, 1961; 0915 MST;
Fade rate 2.5 cps; S/N 26 db; Rhombic antenna

E 19.247 Mc/s; August 14, 1961; 1339 MST
Fade rate 0.5 cps; S/N 36 db; Rhombic antenna

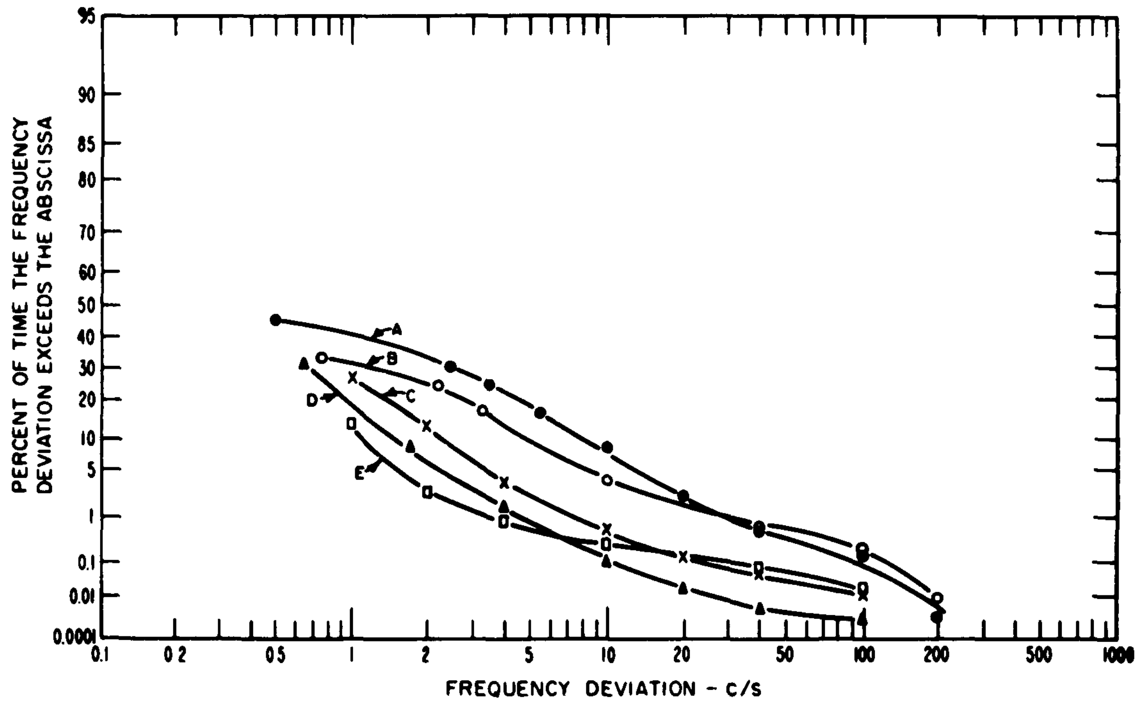

Figure 19. Cumulative distributions of frequency deviations

A 14.688 Mc/s; August 10, 1961; 0952 MST; Fade rate 6 cps; S/N 17 db; Dipole antenna

B 19.247 Mc/s; August 21, 1961; 0737 MST; Fade rate 1.25 cps; S/N 21 db, Dipole antenna

C 14.688 Mc/s; August 16, 1961; 1040 MST; Fade rate 2 cps; S/N 22 db, Rhombic antenna

D 14.688 Mc/s; August 16, 1961; 0840 MST; Fade rate 1.25 cps; S/N 37 db; Dipole antenna

E 14.688 Mc/s; August 17, 1961; 1353 MST; Fade rate < 1cps, S/N 25 db; Dipole antenna

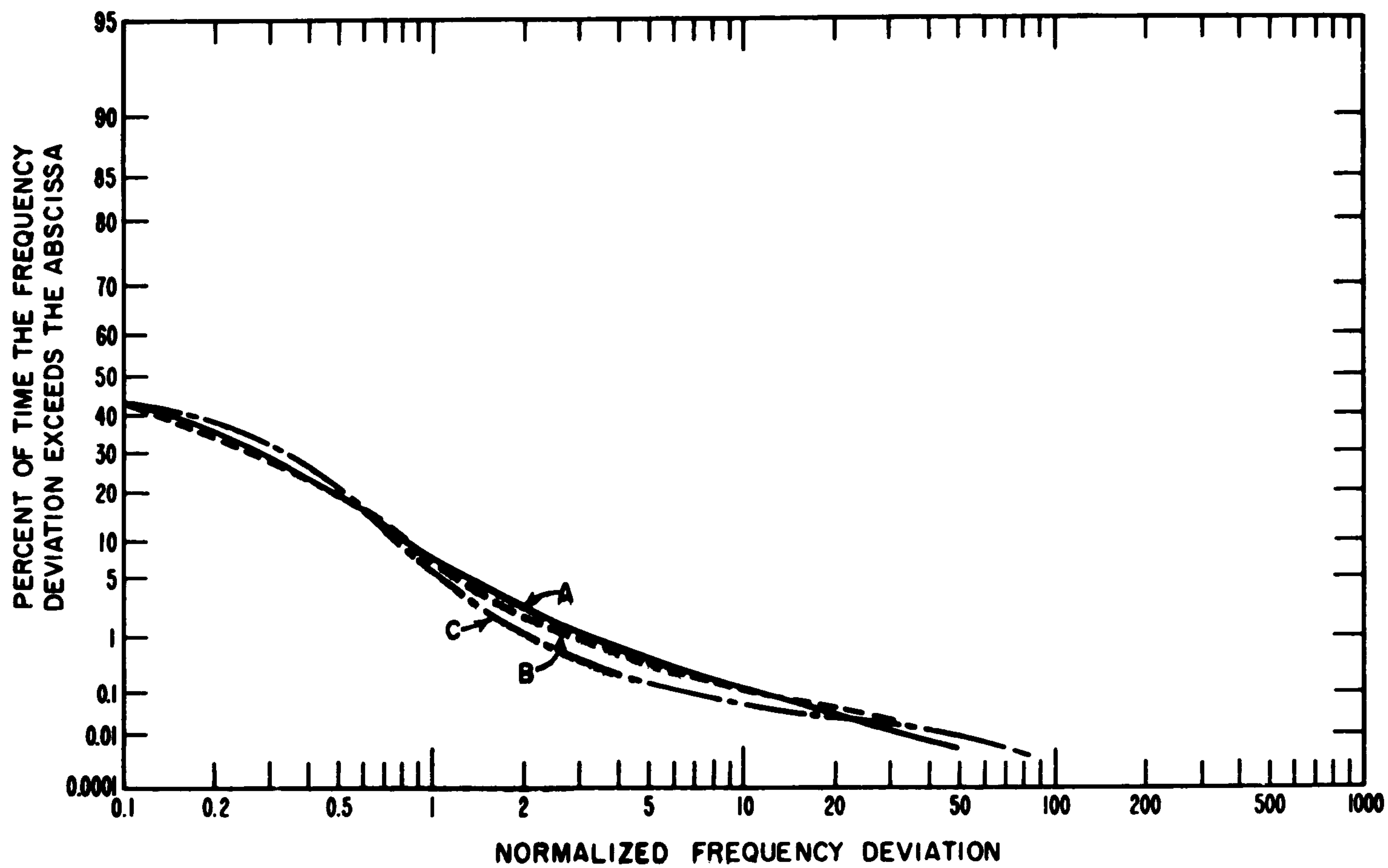

Figure 20. Comparison of theoretical and normalized measured frequency deviation distribution curves

A Theoretical curve

B Normalized experimental curve - good fit

C Normalized experimental curve - poor fit

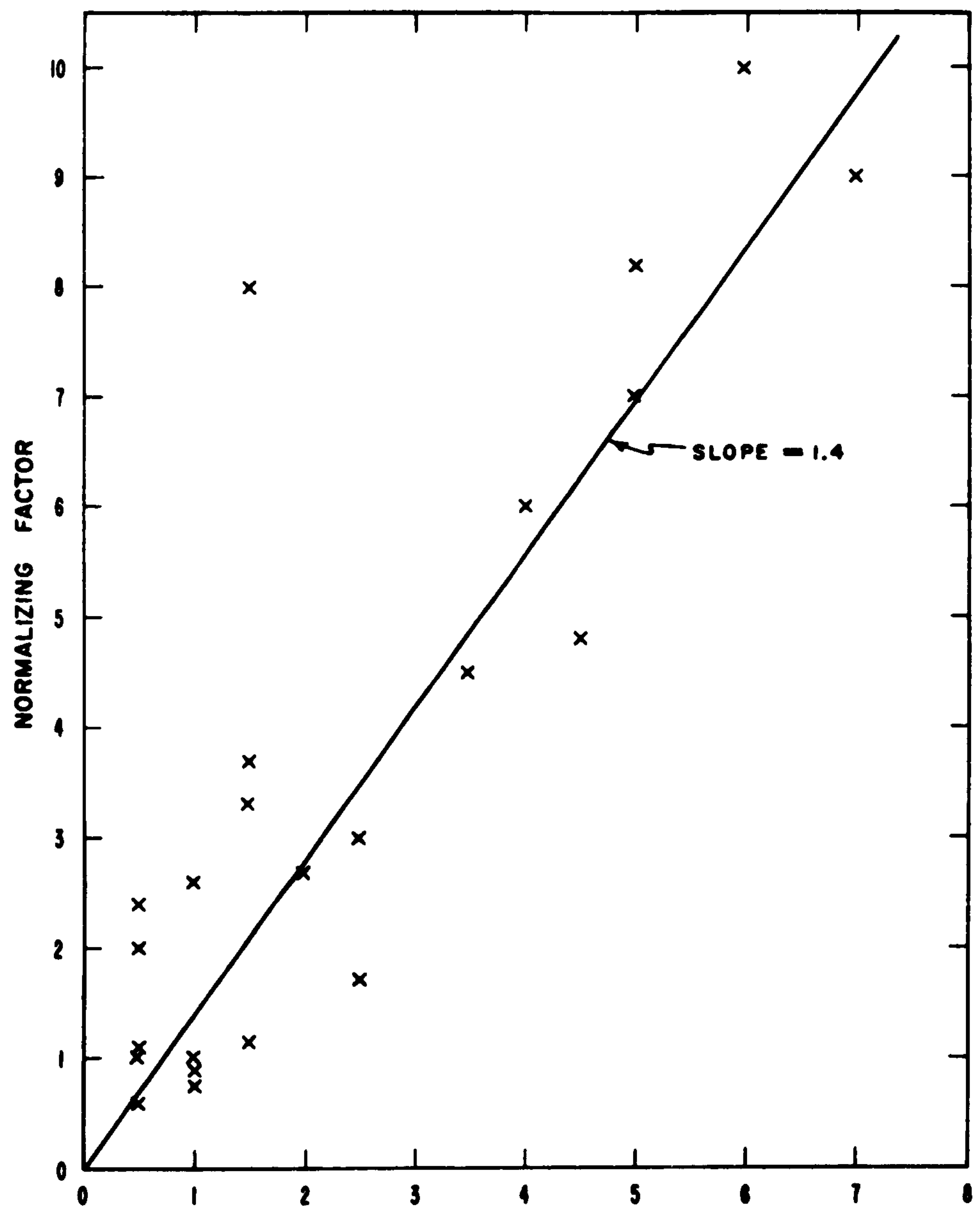

Figure 21. Comparison of experimentally determined normalizing factor with the observed fading rate

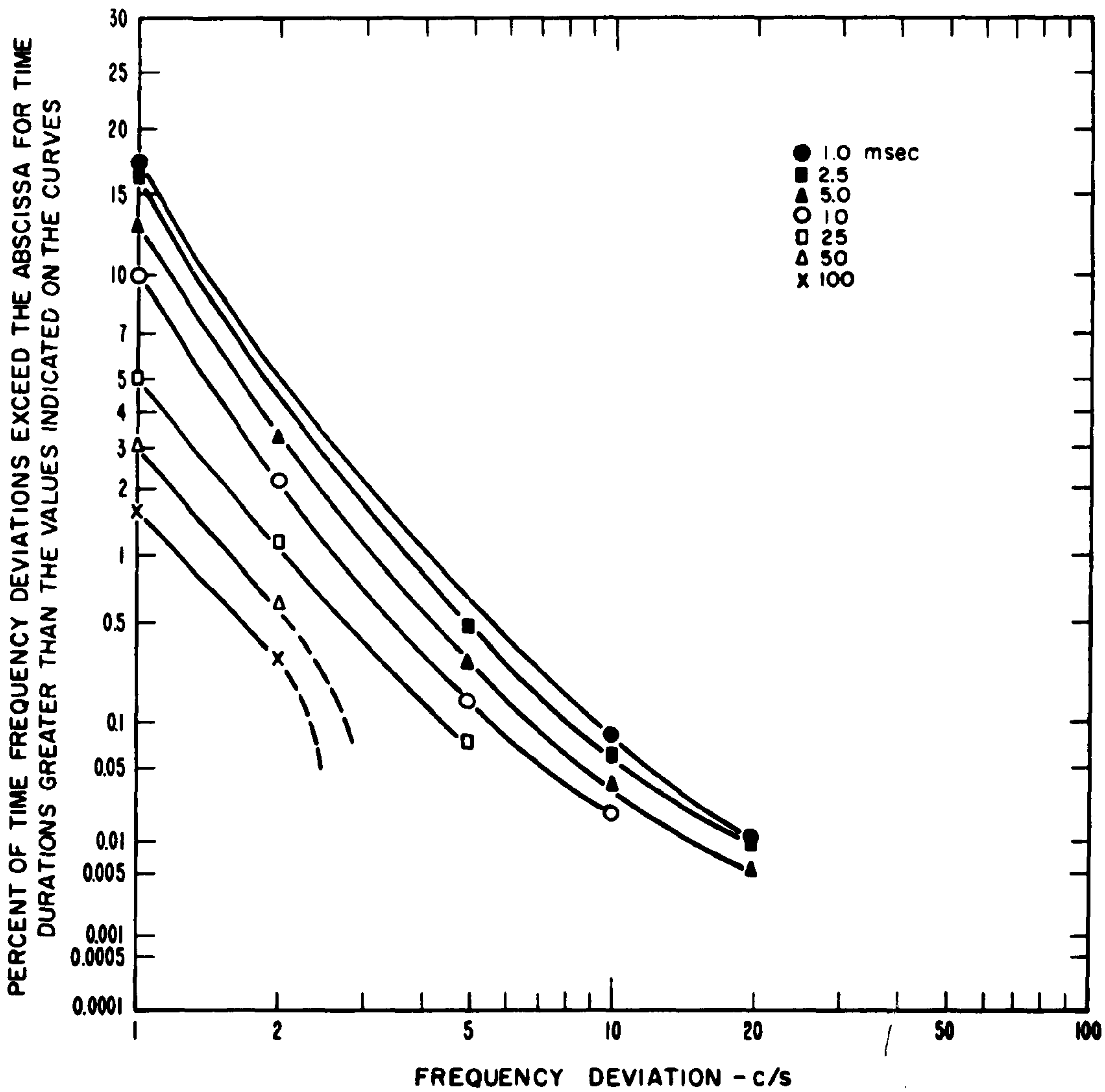

Figure 22. Distributions of frequency deviations for various minimum durations.
19, 247 Mc/s; August 9, 1961; 1308 MST
Fade rate < 1 cps; S/N 55 db; Dipole antenna

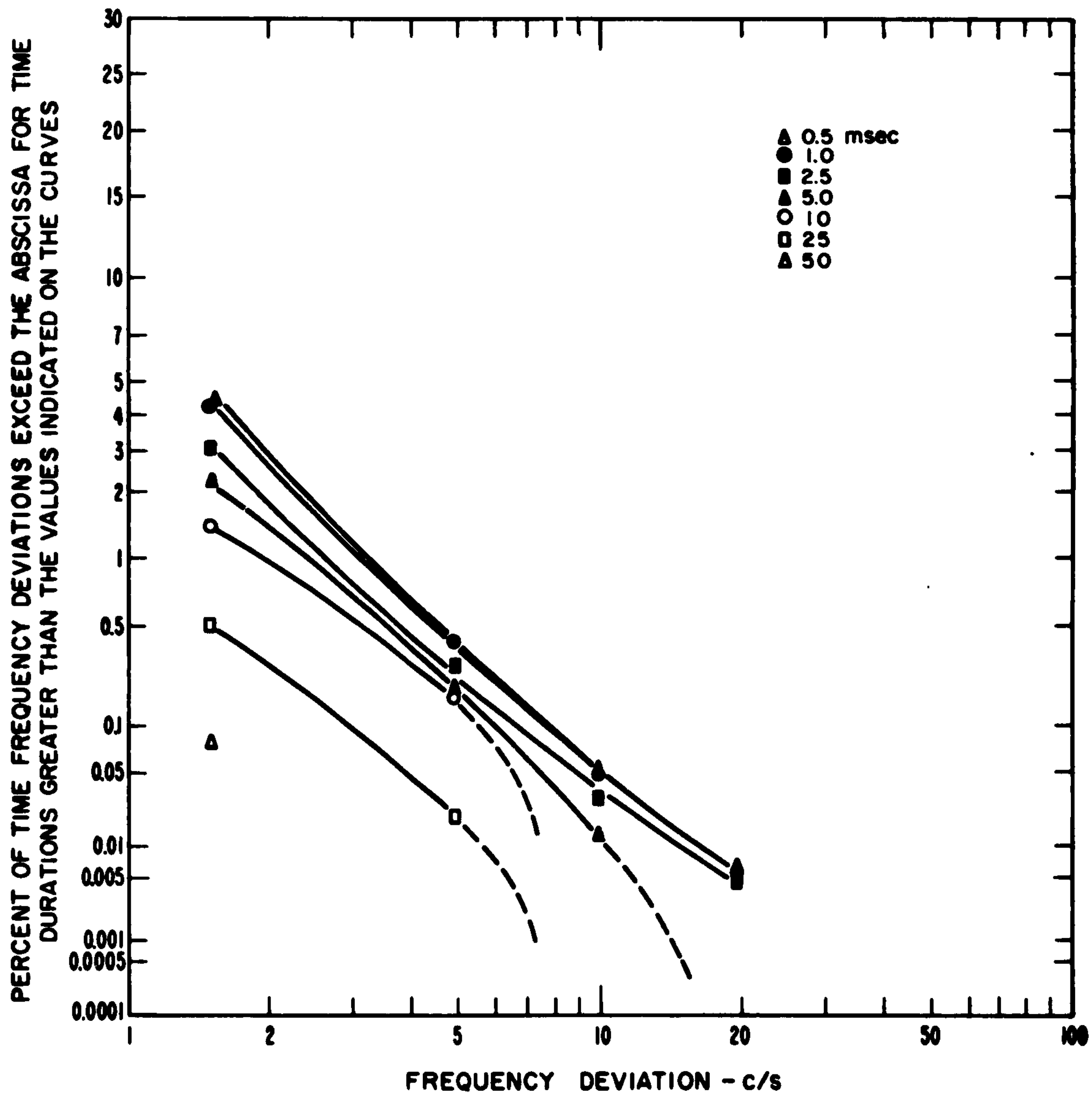

Figure 23. Distributions of frequency deviations for various minimum durations
14.688 Mc/s; August 9, 1961; 1548 MST
Fade rate 1 cps; S/N 20 db; Rhombic antenna

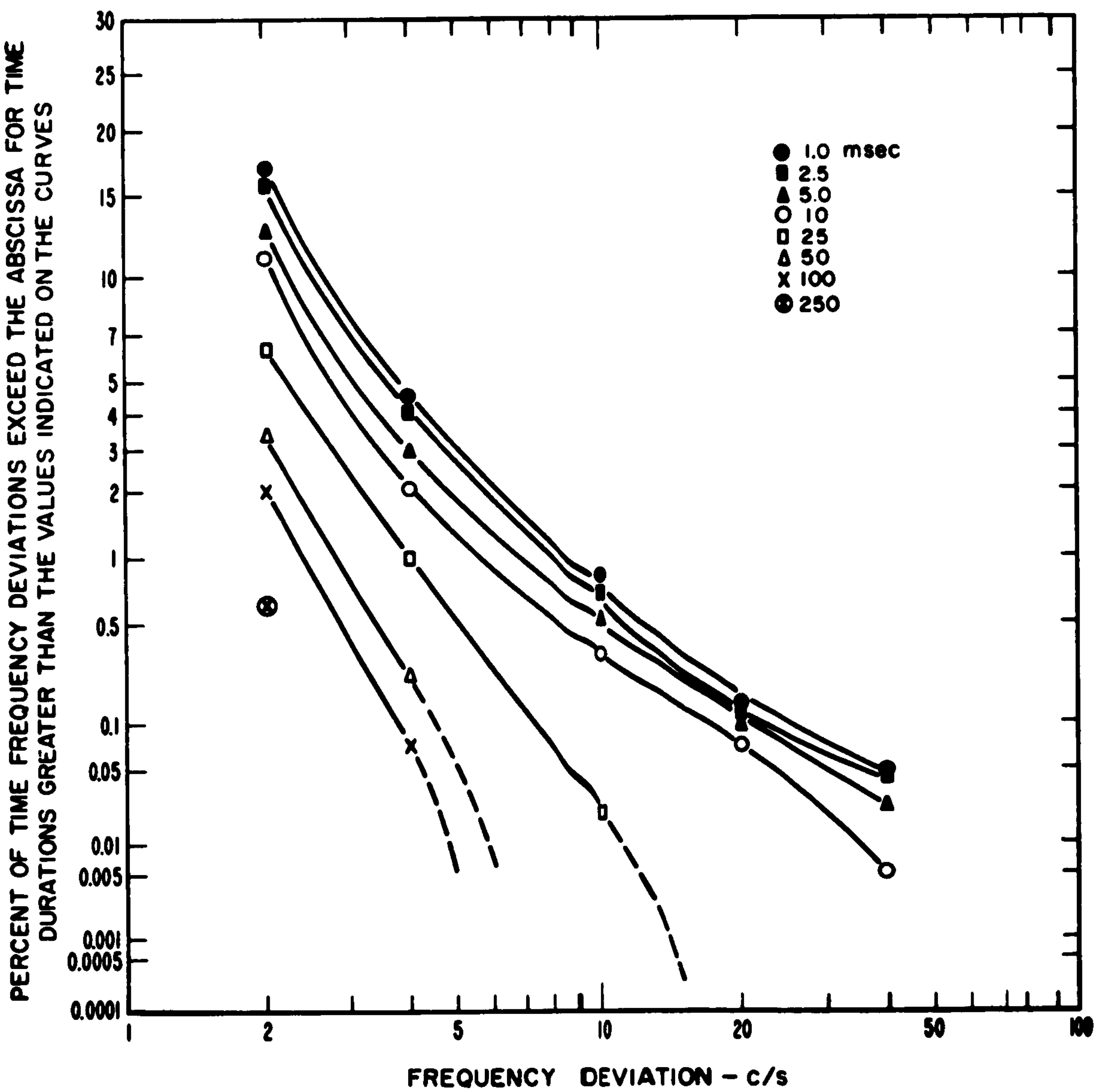

Figure 24. Distributions of frequency deviations for various minimum durations
14.688 Mc/s; August 16, 1961; 1040 MST
Fade rate 2 cps; S/N 22 db; Rhombic antenna

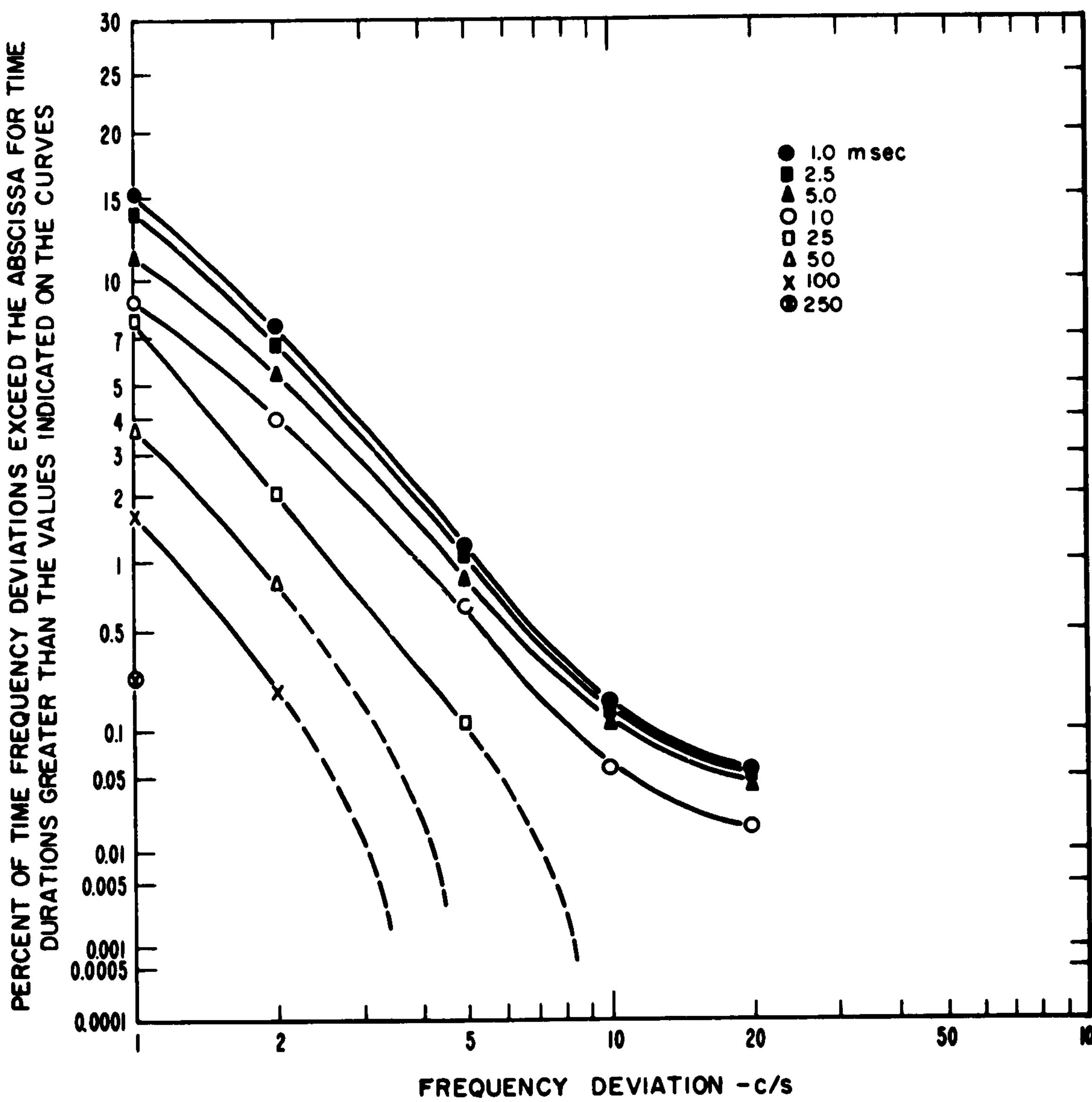

Figure 25. Distributions of frequency deviations for various minimum durations
14.688 Mc/s; August 15, 1961; 0915 MST
Fade rate 2.5 cps; S/N 26 db; Rhombic antenna

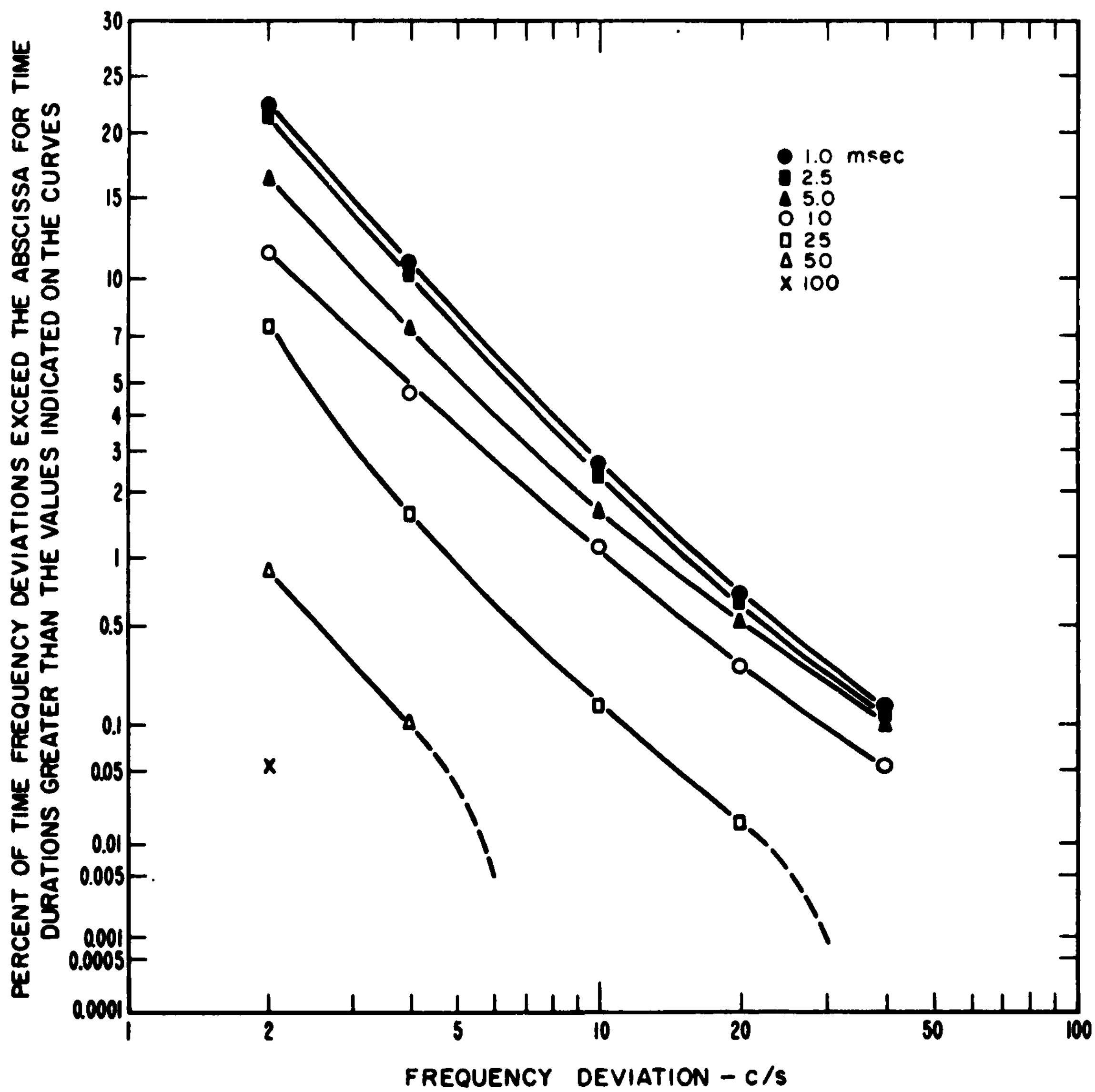

Figure 26. Distributions of frequency deviations for various minimum durations
14.688 Mc/s; August 23, 1961; 0540 MST
Fade rate 3 cps; S/N 19 db; Dipole antenna

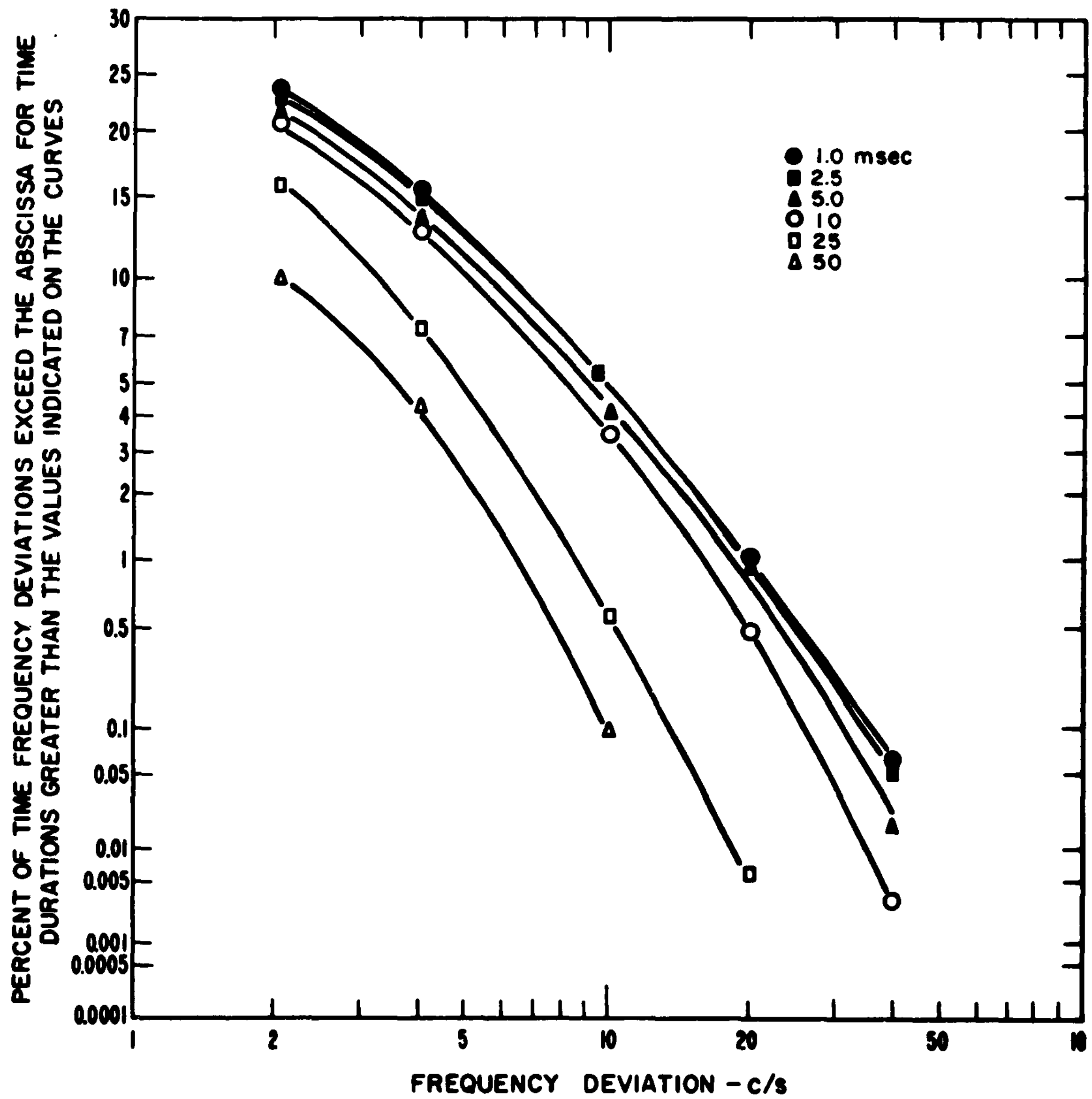

Figure 27. Distributions of frequency deviations for various minimum durations
14.688 Mc/s; August 11, 1961; 2037 MST
Fade rate 4 cps; S/N 30 db; Rhombic antenna

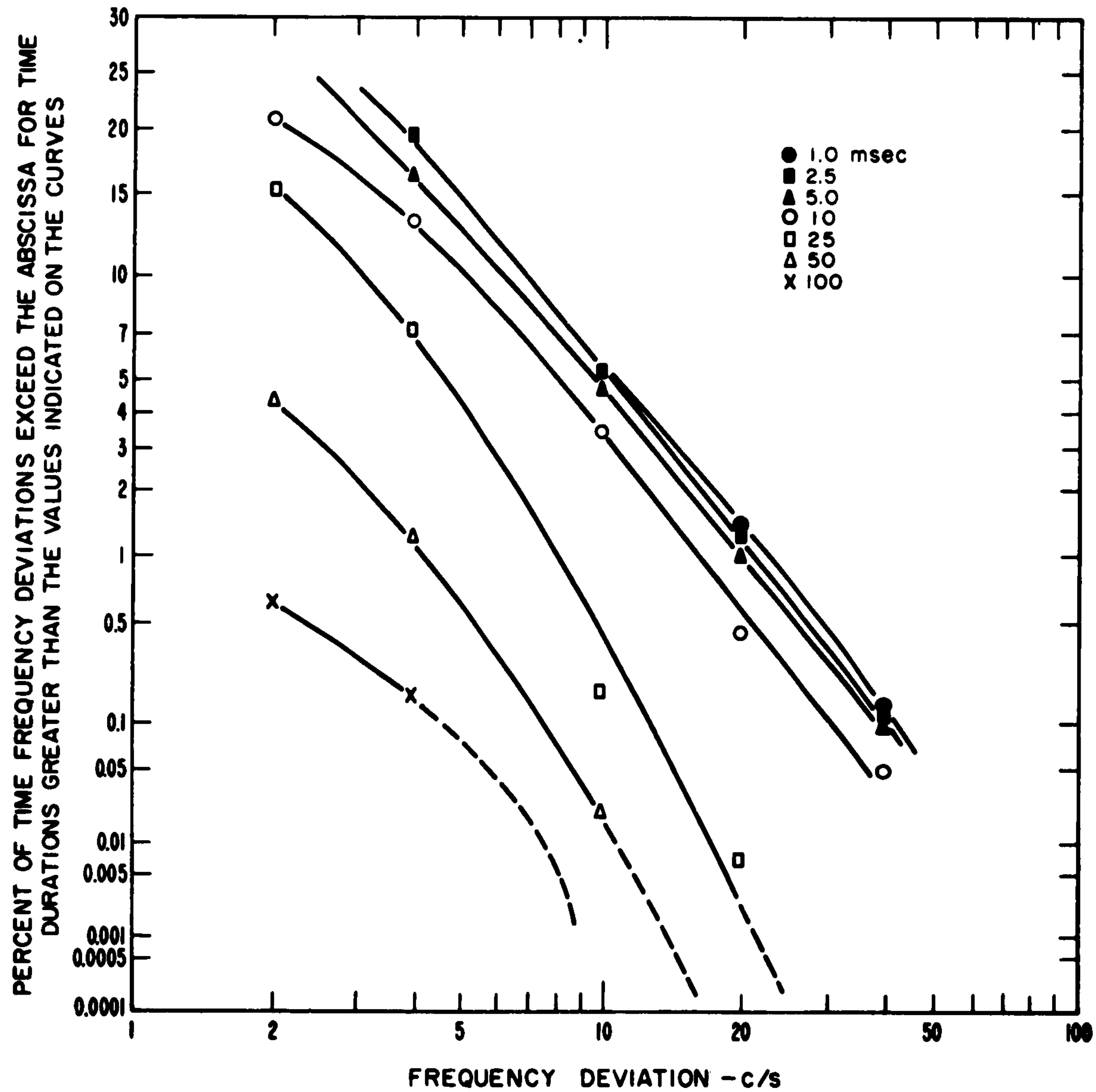

Figure 28. Distributions of frequency deviations for various minimum durations
14.688 Mc/s; August 10, 1961; 1000 MST
Fade rate 5 cps; S/N 25 db; Rhombic antenna

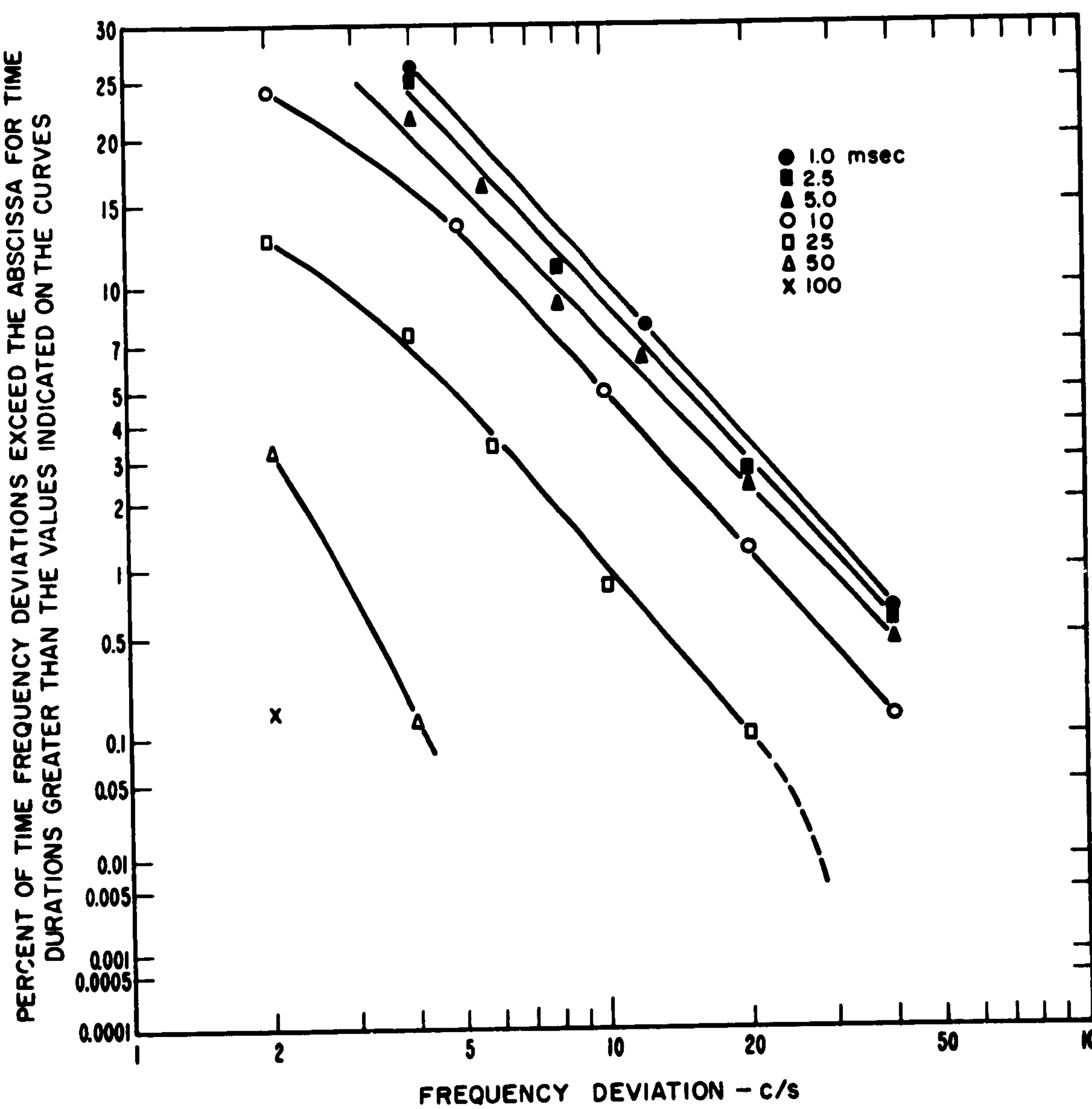

Figure 29. Distributions of frequency deviations for various minimum durations
14.688 Mc/s; August 10, 1961; 0952 MST
Fade rate 6 cps; S/N 17 db; Dipole antenna

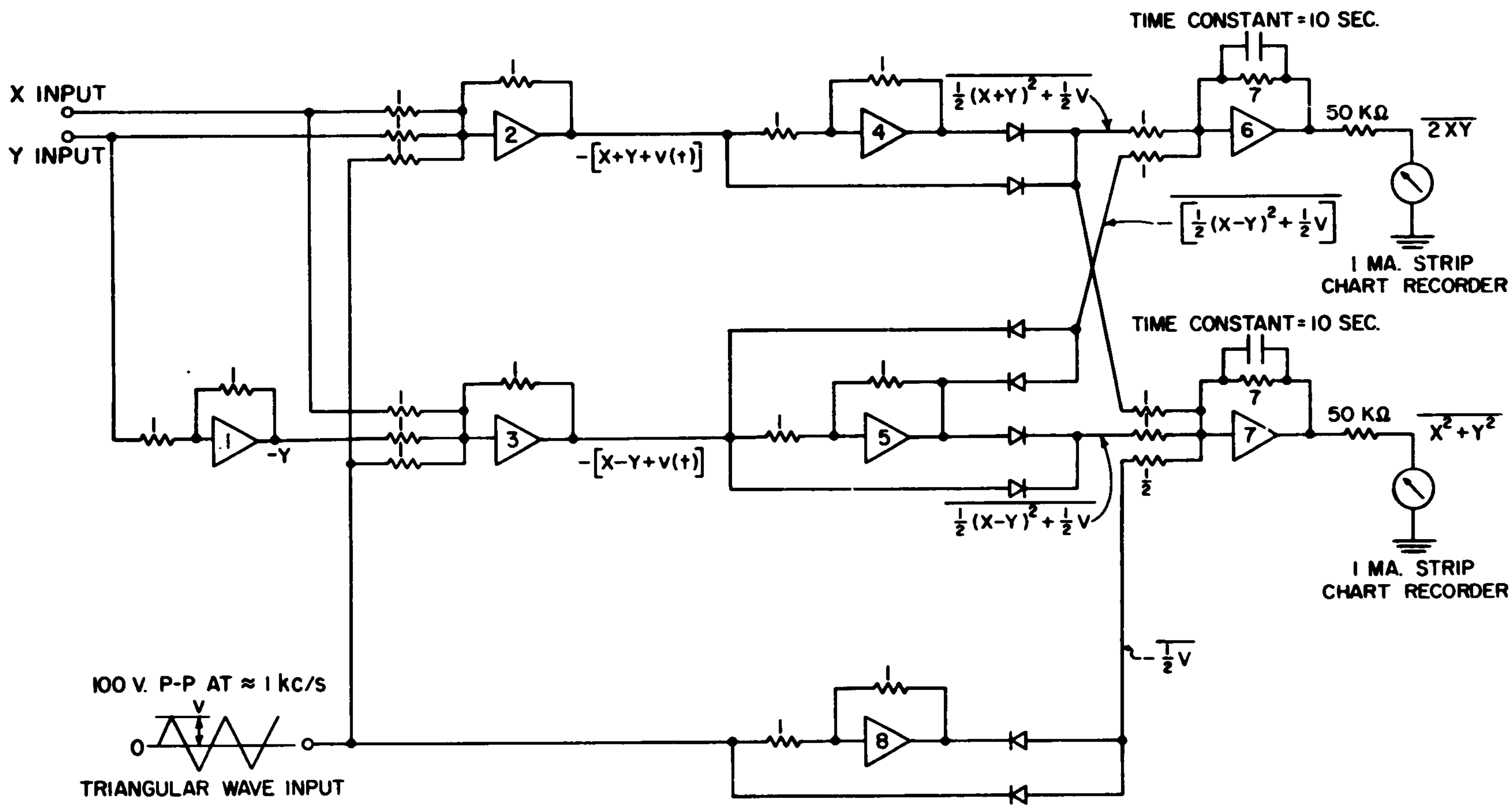

Figure 30. **Block diagram of electronic correlator**

☆ U.S. GOVERNMENT PRINTING OFFICE : 1963 O—670639

U. S. DEPARTMENT OF COMMERCE
Luther H. Hodges, *Secretary*

NATIONAL BUREAU OF STANDARDS
A. V. Astin, *Director*

THE NATIONAL BUREAU OF STANDARDS

The scope of activities of the National Bureau of Standards at its major laboratories in Washington, D.C., and Boulder, Colorado, is suggested in the following listing of the divisions and sections engaged in technical work. In general, each section carries out specialized research, development, and engineering in the field indicated by its title. A brief description of the activities, and of the resultant publications, appears on the inside of the front cover.

WASHINGTON, D. C.

Electricity. Resistance and Reactance. Electrochemistry. Electrical Instruments. Magnetic Measurements. Dielectrics. High Voltage.

Metrology. Photometry and Colorimetry. Refractometry. Photographic Research. Length. Engineering Metrology. Mass and Scale. Volumetry and Densimetry.

Heat. Temperature Physics. Heat Measurements. Cryogenic Physics. Equation of State. Statistical Physics.

Radiation Physics. X-ray. Radioactivity. Radiation Theory. High Energy Radiation. Radiological Equipment. Nucleonic Instrumentation. Neutron Physics.

Analytical and Inorganic Chemistry. Pure Substances. Spectrochemistry. Solution Chemistry. Standard Reference Materials. Applied Analytical Research. Crystal Chemistry.

Mechanics. Sound. Pressure and Vacuum. Fluid Mechanics. Engineering Mechanics. Rheology. Combustion Controls.

Polymers. Macromolecules: Synthesis and Structure. Polymer Chemistry. Polymer Physics. Polymer Characterization. Polymer Evaluation and Testing. Applied Polymer Standards and Research. Dental Research.

Metallurgy. Engineering Metallurgy. Microscopy and Diffraction. Metal Reactions. Metal Physics. Electrolysis and Metal Deposition.

Inorganic Solids. Engineering Ceramics. Glass. Solid State Chemistry. Crystal Growth. Physical Properties. Crystallography.

Building Research. Structural Engineering. Fire Research. Mechanical Systems. Organic Building Materials. Codes and Safety Standards. Heat Transfer. Inorganic Building Materials. Metallic Building Materials.

Applied Mathematics. Numerical Analysis. Computation. Statistical Engineering. Mathematical Physics. Operations Research.

Data Processing Systems. Components and Techniques. Computer Technology. Measurements Automation. Engineering Applications. Systems Analysis.

Atomic Physics. Spectroscopy. Infrared Spectroscopy. Far Ultraviolet Physics. Solid State Physics. Electron Physics. Atomic Physics. Plasma Spectroscopy.

Instrumentation. Engineering Electronics. Electron Devices. Electronic Instrumentation. Mechanical Instruments. Basic Instrumentation.

Physical Chemistry. Thermochemistry. Surface Chemistry. Organic Chemistry. Molecular Spectroscopy. Elementary Processes. Mass Spectrometry. Photochemistry and Radiation Chemistry.

Office of Weights and Measures.

BOULDER, COLO.

Cryogenic Engineering Laboratory. Cryogenic Equipment. Cryogenic Processes. Properties of Materials. Cryogenic Technical Services.

CENTRAL RADIO PROPAGATION LABORATORY

Ionosphere Research and Propagation. Low Frequency and Very Low Frequency Research. Ionosphere Research. Prediction Services. Sun-Earth Relationships. Field Engineering. Radio Warning Services. Vertical Soundings Research.

Radio Propagation Engineering. Data Reduction Instrumentation. Radio Noise. Tropospheric Measurements. Tropospheric Analysis. Propagation-Terrain Effects. Radio-Meteorology. Lower Atmosphere Physics.

Radio Systems. Applied Electromagnetic Theory. High Frequency and Very High Frequency Research. Frequency Utilization. Modulation Research. Antenna Research. Radiodetermination.

Upper Atmosphere and Space Physics. Upper Atmosphere and Plasma Physics. High Latitude Ionosphere Physics. Ionosphere and Exosphere Scatter. Airglow and Aurora. Ionospheric Radio Astronomy.

RADIO STANDARDS LABORATORY

Radio Physics. Radio Broadcast Service. Radio and Microwave Materials. Atomic Frequency and Time-Interval Standards. Radio Plasma. Millimeter-Wave Research.

Circuit Standards. High Frequency Electrical Standards. High Frequency Calibration Services. High Frequency Impedance Standards. Microwave Calibration Services. Microwave Circuit Standards. Low Frequency Calibration Services.